FIT FOR SPACE: LEVERAGING A NOVEL SKIN CONTACT MEASUREMENT TECHNIQUE TOWARD A MORE EFFICIENT LIQIUID COOLED GARMENT

A Thesis
SUBMITTED TO THE FACULTY OF
UNIVERSITY OF MINNESOTA
BY

Crystal Marie Compton

IN PARTIAL FULFILLMENT OF THE REQUIREMENTS
FOR THE DEGREE OF
MASTER OF SCIENCE

Dr. Lucy E. Dunne

August 2016

Abstract

Comfort, mobility, and performance are all affected by the fit and contour of a garment to the body. Understanding the body-garment relationship allows for improvement of all of these aspects, and thus the garment and experience for the wearer. With current methods, it is possible to measure the body-garment relationship primarily in static positions, but mobile analysis is time- and equipment-intensive. A more direct garment contour and body contact monitoring procedure would benefit the functional clothing design community. Mobile measurement is especially important for functional garments, as the body-garment relationship changes over time during body movements. Here, we describe a new method developed to measure the body-garment relationship, specifically for mobile scenarios. This method detects body-garment contact using an electrical signal within a circuit formed between the garment and the body. The analog electrical connection (expressed as a varying voltage using a voltage-divider circuit) between the body and a conductive patch is processed and recorded by a microcontroller.

In this investigation three main variables were evaluated for their influence on the measurement of body-garment contact: 1) patch materials, 2) applied force, and 3) patch sizes were tested within the body/garment interface. Material results showed that all of the tested materials (with the exception of one material, which contained the sparsest surface area of conductive material) facilitated a voltage response in the presence of body contact that could be viable for detecting contact between body and garment. However, preliminary tests revealed that materials with lower resistivity and more rigid structure

facilitated a smoother signal with less noise, which correlated more closely with the input signal. Applied force results showed that the amount of force between the sensor and the body affects the response of the system. All patch sizes with the exception of the smallest size tested (0.3175 cm) were effective in measuring body-garment contact. The smallest diameter possible for the conductive patch is of interest, in an attempt to minimize its effect on the body-garment measuring system.

A 0.635 cm diameter conductive hook fastener sensor was subsequently used to implement this method in a pilot evaluation of LCG (Liquid Cooling Garment) fit. A grid of six analog sensors (maximum amount for microcontroller used) was integrated into the right torso region of the LCG for testing. Various movements that would be similar to movements that astronauts would be performing in EVA were used to test body-garment contact. Results show distinct differences in body contact for each sensor during each movement.

Table of Contents

List of Tables

List of Figures

Nomenclature

LCG	=	Liquid Cooling Garment
LCVG	=	Liquid Cooling and Ventilation Garment
EMU	=	Extravehicular Mobility Unit
EVA	=	Extravehicular Activity
TMG	=	Thermal Micrometeoroid Garment
PLSS	=	Primary/Portable Life Support System
TCU	=	Thermal Comfort Undergarment
LoNE	=	Lines of Non-Extension
JSC	=	Johnson Space Center
3-D	=	three-dimensional
V	=	volts
MΩ	=	megaohm
MHz	=	megahertz
Hz	=	hertz
Sq.	=	square

CHAPTER 1: INTRODUCTION

The relationship between a garment and the wearer's body can be a complex interaction but very important for many functional garments. Understanding this relationship in the design process has important implications on the wearer's comfort, success of the garment, and much more. Gaining a better understanding of the dynamic between the two can provide insights that lead to a better designed and fitted garment.

For example, one garment that is highly affected by the body to garment relationship is the liquid cooling garment/liquid cooling and ventilation garment (LCG/LCVG), which is part of the Extravehicular Mobility Unit (EMU) spacesuit worn by astronauts. This garment is a fundamental mechanism used to regulate astronaut's core body temperature during launch, landing, and extravehicular activity (EVA), and relies on conduction as a means of thermal transport. Therefore, in order to work effectively, it needs to be in close contact with the body at all times. Although it is anecdotally known that body-garment contact problem areas exist in the LCG/LCVG, it's unknown where exactly these problem areas are, or how they change during body movement.

Traditional methods of measuring the relationship between the body and garment rely primarily on 3-D body scanning. These methods provide valuable data about this relationship, however, they are also limited to only testing in static positions and can be significantly expensive in equipment costs. Due to the fact that the LCG/LCVG has a layout of tubes that are more rigid than the textile they are attached to, the tubes can pull away from and come out of contact with the body during various movements, an effect that would not be adequately captured in a static measurement. Mobile measurement is

especially important for functional garments, as the body-to-garment relationship changes over time. It would be valuable to have a low-cost, easy method to effectively measure areas of contact and noncontact in a functional garment, while the wearer is moving.

This thesis describes a new method developed to measure the body-to-garment relationship, specifically for mobile scenarios. It is based on a 'switch'-like principle, in which contact with the grounded body completes a circuit, allowing current to flow to the analog input of a microcontroller. It is designed to provide data about the body-to-garment relationship, and more specifically, to measure whether the garment is in contact with the body or not and when. Various conductive materials, sizes, and contact forces were initially tested for their effectiveness in creating a reliable electrical representation of the body/garment contact signal in this study. The conductive material with the most reliable and sensitive response within the developed system and the smallest patch size viable for this method has been used for this study. This system was implemented into an LCG provided by the Advanced Spacesuit Team Lab at Johnson Space Center (JSC) for testing body-garment relationship in the right torso region of the body. Six analog sensors were used for testing this method in the LCG. Results show averages of the amount of contact time for each sensor tested during a series of body movements corresponding to EVA-like task activities.

CHAPTER 2: BACKGROUND

2.1 EMU Spacesuit

The EMU spacesuit is used for EVA or spacewalks that take place outside of the spacecraft. Due to the extreme environments in space, the EMU spacesuit is an essential component, as it provides the needed protection for the astronaut to go outside of the spacecraft and stay alive in the vacuum of space (MSFC, 2013). The EMU spacesuit does not allow thermal energy to flow freely during EVA, because it is a completely encapsulated environment.

The EMU spacesuit is comprised of 14 different layers that heavily insulate the wearer with a series of strong and reflective materials (Figure 2.1) (Vogt, 1998). These layers of insulation protect the astronaut from the extreme environments in space. Although these layers provide many life-saving benefits and are vitally needed, they also can create an unfavorable amount of heat build-up and accumulation of moisture, as body heat and sweat have nowhere to be released to (because the EMU spacesuit traps air and body heat inside and cannot release energy to the outside environment).

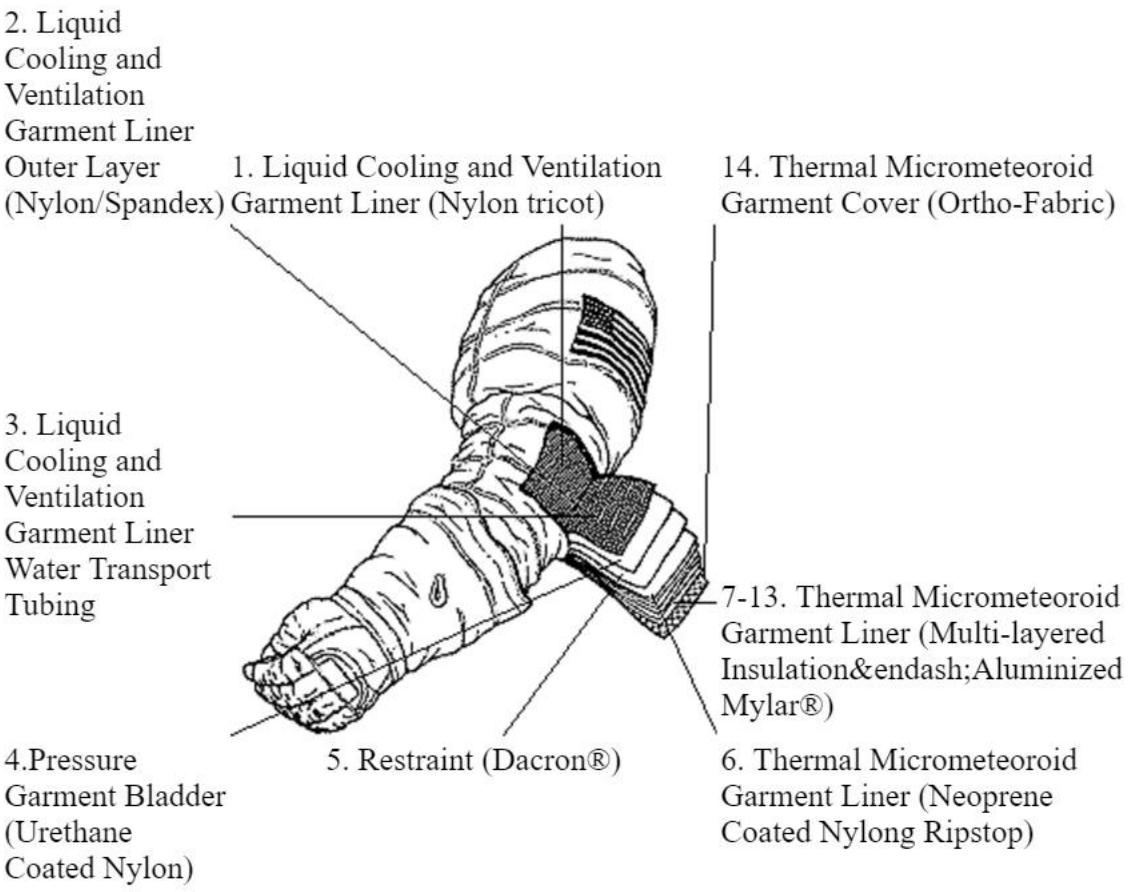

Figure 2.1: Layers of the EMU spacesuit.

(James, 2016)

Astronauts are protected from the extreme variation of temperatures in space by the thermal micrometeoroid garment (TMG), which makes up 7 outer layers of the EMU spacesuit (Vogt, 1998). The inside layers are made using aluminized Mylar®, laminated with Dacron® scrim (James, 2016). The TMG protects the wearer from the sun's heat and from extreme cold in the shade, however, during this process it keeps the body heat in as well ("Extravehicular Activity (EVA) Thermal Micrometeoroid Garment (TMG) Thermal Performance Study," 1996). This results in both good and bad outcomes: it

keeps the wearer safe from extreme temperatures, but also keeps the heat from the body in the inside environment of the spacesuit. When atmospheric temperatures (inside the spacesuit) are high, accumulating too much body heat within the spacesuit can result in discomfort, overheating, accumulating excess sweat, and dehydration, and more (Strauss, Krog, & Feiveson, 2005).

2.2 Human Body

The human body produces heat when it moves or exerts energy (Fiala, Lomas, & Stohrer, 1999). When the body's temperature increases, information is sent to the brain (hypothalamus, often referred to as the body's thermostat and controls thermoregulation), which then sends signals to activate the body's natural cooling system (through sweating and vasodilation), in an attempt to cool the body to a comfortable temperature (Hensel, 1973).

Sweating is one of the first methods the body will use to cool itself. Sweat is produced by the body's sweat glands which release liquid (sweat) to the skin surface (Arens & Zhang, 2006). This liquid is typically free (if not in an encapsulated environment) to evaporate off of the skin, thus cooling the body by phase change.

Vasodilation happens when the body's blood vessels under the skin surface dilate, which increases the amount of blood flow and releases heat through convection, conduction, and radiation.

Thermoregulation of the body to achieve and maintain a comfortable and safe core internal temperature (homeostasis) (Fiala et al., 1999) is often a combination of these body processes and on-body technologies like traditional clothing or garments with

augmented functionality. The LCG/LCVG is a garment with augmented functionality that astronauts wear for launch, entry, and EVA and is meant to help them maintain thermal balance while inside of a spacesuit. This garment manages the thermal energy created by the body, to ultimately regulate the body's core temperature and maintain a comfortable and safe working environment.

The LCG/LCVG relies on conduction, which is the transfer of heat/energy from one object to another object, as it is a primary means of regulating body temperature and managing the thermal energy produced by the body. Heat from the body is conducted to a garment that typically contains cold flowing water (Figure 2.2). These types of garments are very useful in high-heat environments or when the body needs to be heavily insulated, because they draw off excess heat from the body when more common thermoregulation mechanisms aren't sufficient (Watkins S. M., 1995). In this case, both are reasons the LCG/LCVG is used to achieve thermoregulation. "It is necessary to provide a means to cool the body of a person who is placed in a heavy, air-tight, protective outer garment such as that used in high altitude and space exploration" (Crocker, 1969).

Figure 2.2: LCVG worn on body.

(Mundo, 2015)

2.3 LCG/LCVG

The LCG/LCVG's primary function is to regulate an astronaut's core body temperature to achieve thermoregulation. This garment is worn as the base layer of the EMU spacesuit (Figure 2.3), with an optional thermal comfort undergarment (TCU) that can be chosen by the astronaut to be worn underneath the LCG/LCVG. It is created to be a closely fitted garment with a layout of tubes that have cool water flowing through the tubes. The tubes, when in contact with the human body, cool the body by conducting heat away from the skin to keep the astronaut at a comfortable and safe temperature while in the encapsulated environment of a spacesuit.

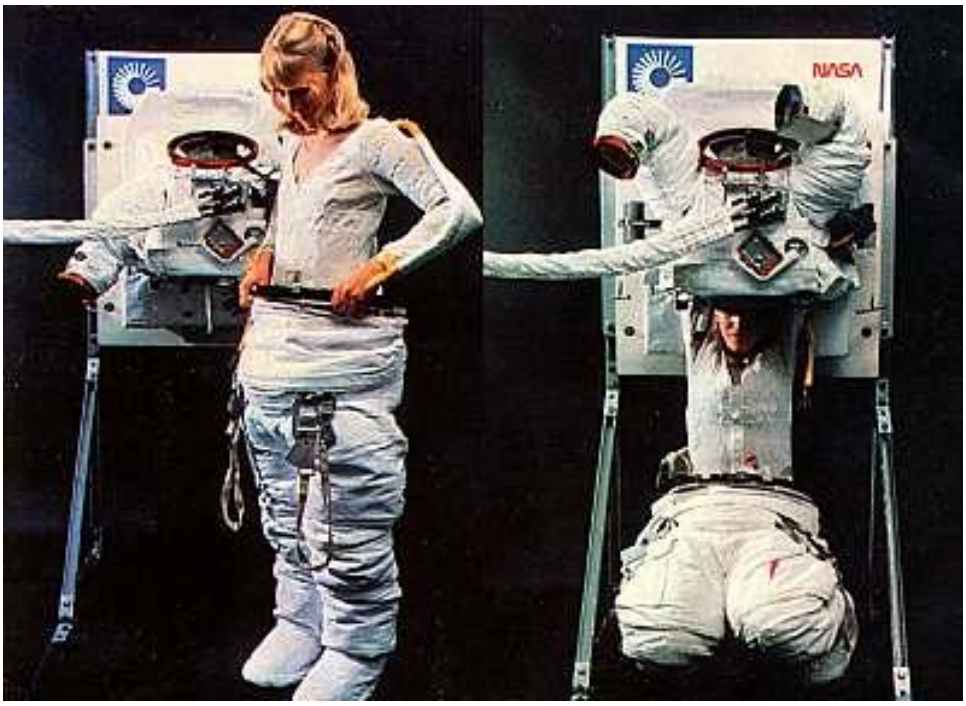

Figure 2.3: Donning EMU spacesuit while wearing LCVG.

(Weber Luk, 2012)

The tubes of the LCG/LCVG are threaded into the garment between two layers of textiles (Figure 2.4). The layer closest to the skin is a 2-way stretch, 100% nylon textile. Directly on top of this layer is a network of Tygon® tubing, made of polyvinyl chloride (PVC), which spans across the entire garment. Finally, the last and top-most layer is a 4-way stretch textile of 100% spandex fiber, mesh construction. The tubes are connected to the top-most mesh layer by weaving them through the open holes of the mesh textile.

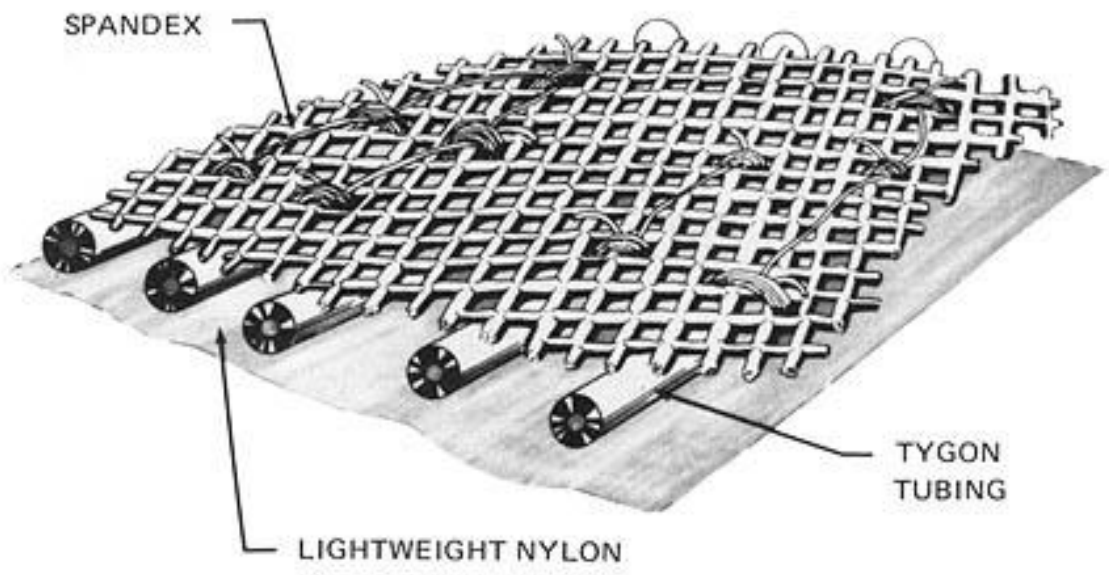

Figure 2.4: LCG/LCVG material layers/construction.

(Carson, Rouen, Lutz, & McBarron, II)

When connected to the primary/portable life support system (PLSS) of the EMU spacesuit, the LCG/LCVG tubes contain cool water that continuously circulates around the body. The LCG/LCVG also contains vents that draw sweat away from the body and recycle it through the water-cooling system, to help facilitate additional cooling (MSFC, 2013). The PLSS is worn on the back of the astronaut, similar to a backpack, and provides the needed elements of survival in space (Figure 2.5). A few of the key elements that the PLSS includes: oxygen, removes carbon dioxide, holds a battery for power, and contains the water-cooling equipment (connected to the LCG/LCVG).

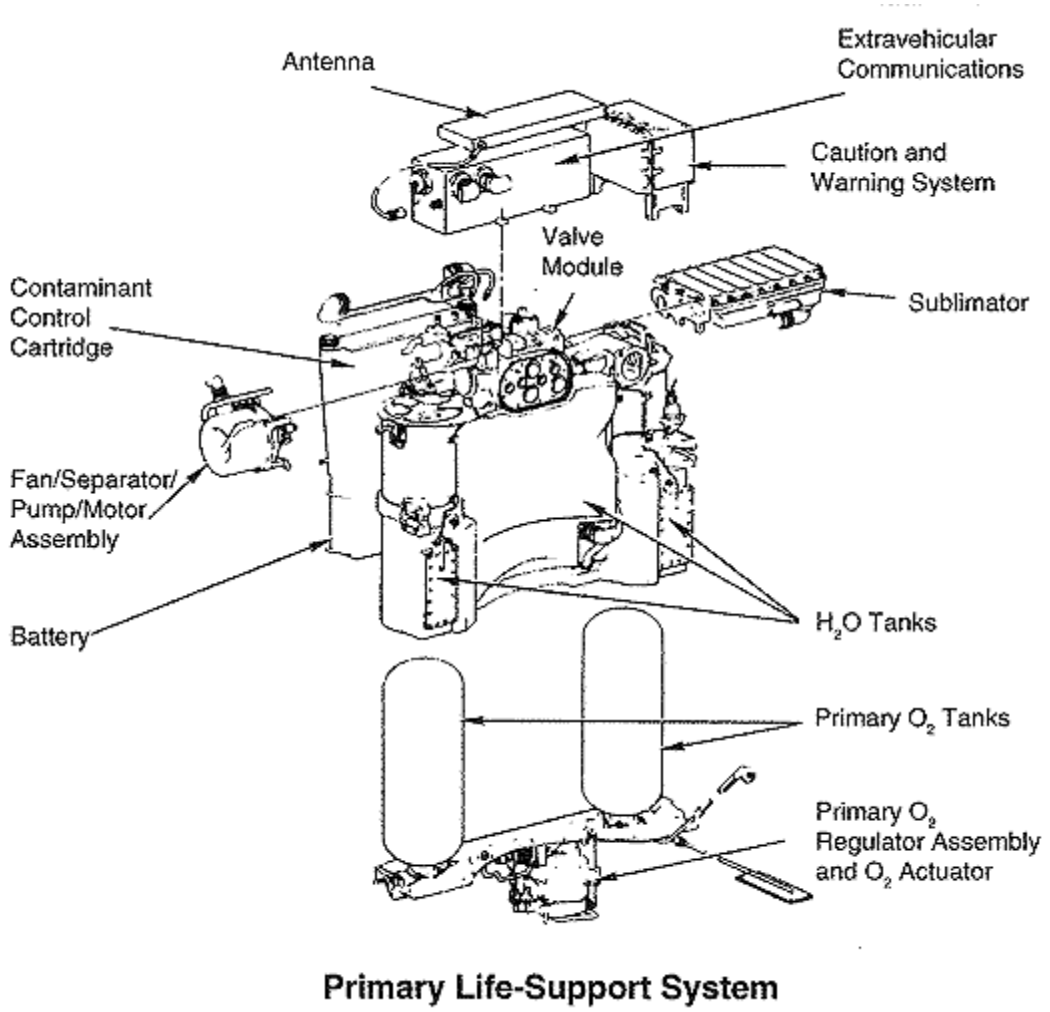

Figure 2.5: Primary Life Support System diagram.

(James, 2016)

To be effective the LCG/LCVG liquid component primarily relies on conduction. The liquid-filled tubes need to be in contact with the body in order to most efficiently draw heat away from the body. Because the LCG/LCVG relies on conduction, the surface contact between the garment (holding the tubes) and the body is crucial. Good thermal conductivity allows for cooling efficiency as well as moisture management (Cao,

Branson, Peksoz, Nam, & Farr, 2006).

Because the tubing integrated into the LCG/LCVG is non-extensible and somewhat stiff, body movements can cause the tubing to buckle away from the skin. An example of this effect is shown in Figure 2.6. This kind of buckling behavior can lead to a decrease in the rate of conductive thermal transport (and therefore thermoregulation in that area of the body).

Figure 2.6: Gaping area on LCG.

It has not been rigorously studied, but is anecdotally known that the LCG/LCVG tubes can lose contact with the body. The tubes are pulled away from the body by forces placed upon the garment (and the tubes) due to body movement, various body positions, and/or an ill-fitting garment. In order to improve contact between the body and the LCG/LCVG, a deeper understanding of this issue is needed, such as: where the garment is losing contact with the body, during what movements or positions, and how fit and material/textile selection plays a role. A direct, cost-effective method of measuring the relationship between the body and the LCG/LCVG would provide information allowing parameters of the design problem to be understood. Ultimately the information could be used to design a more effective and safe LCG/LCVG.

2.4 Functional Clothing Fit

Functional clothing design is a branch of clothing design that is user-requirement specific and focuses on meeting the performance requirements of a user in extreme conditions (Gupta, 2011). A flow chart showing the design process of functional clothing is illustrated below in Figure 2.7. This approach is useful in the designing and development of the LCG/LCVG, as the focus for these garments is on the performance needs of regulating the body's core temperature while in the extreme conditions of space.

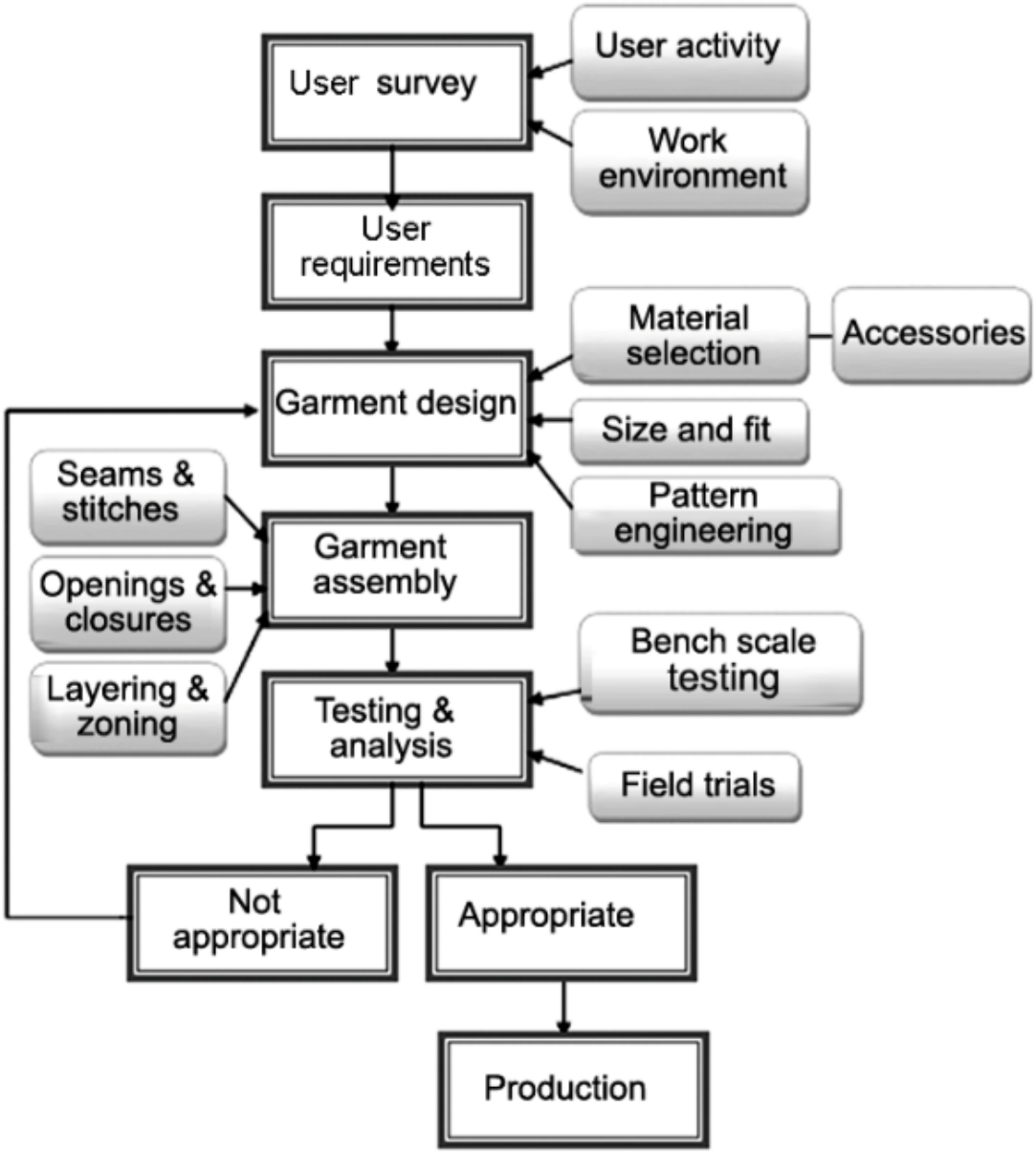

Figure 2.7: Functional clothing design flow chart.

(Gupta, 2011)

Fit is the specific relationship of the garment's dimensions to the body's dimensions. Variability in body dimensions (anthropometrics) across a population can

make it difficult to mass-produce garments that fit an entire population effectively (Gupta & Zakaria, 2014). Adjustability built into a design can allow a smaller number of sizes to fit a larger range of users, but in the case of the LCG/LCVG this adjustability must also take into account the areas of the garment in which tubing must be held closely to the body, and the directions in which force can be applied to achieve this goal without compromising mobility.

As with any garment, including the LCG/LCVG, an important factor is the change in body dimensions that happen during movement. A garment may fit effectively in one position, but as areas of the body expand and contract during movement the fit relationship changes.

For example, when the knee is bent, the skin surface of the ventral kneecap elongates, and correspondingly contracts along the dorsal knee. Stretch is one method commonly used to maintain fit during movement, but in the case of the LCG/LCVG stretch can be impeded in areas where inextensible tubes are integrated. Tube placement that allows stretch in areas of body expansion can accommodate lengthening changes, but on the opposite side of a joint excess fabric and bulk can be created, resulting in bunching fabric and difficulty bending the leg (Watkins, 1995). Further, this excess fabric may inadvertently pull the LCG/LCVG tubing away from the body during movement. A method to measure and understand the relationship of the body to a garment would be a valuable tool to evaluate garment design options using a functional clothing design approach. The goal is to identify poor fit areas, and thus poor effectiveness of a functional garment.

2.5 Current Methods

2.5.1 Body Scanning

The most common methods used today to understand the relationship between the body and a garment rely on (3-D) body scanning. Typically, two scans are taken, one "nude" (or in underwear) and one clothed scan, which are later superimposed for analysis of air gaps. Several studies have used this method to understand the effects of air gaps on thermal and protective garments, discussed below.

A study by Kim, Lee, Li, Corner, & Paquette (2002) investigated the air gaps found in protective clothing. They quantify the size of the air gaps in single and multilayer garments, dressed on a thermal mannequin. Data were collected by first scanning a nude mannequin, followed by a second scan of a clothed mannequin. The two scans were superimposed and aligned by using an area of both the scans that did not change. Cross-sections of the superimposed scans were taken along the vertical axis. Cross-sections illustrate two contours (from the two scans) that are either superimposed or are separated by a variable distance. The difference in distance calculated between these two contour lines is the air gap in that area.

A study done by Xu & Zhang (2009) studied the "vacant distance ease relation" between the body and a garment. This study also measures air gaps, by calculating the air gap in firefighter fireproof uniforms. Emphasis was on the ease relationship and the specific style of a garment in different sizes. The goal of the study was to define the garment ease in a mathematical manner, as the shortest distance measured from the body surface to the inner surface of the garment in a horizontal direction.

A challenge in functional garment fit is that male and female anatomics are

different, however, many functional garments are fitted to a male form. Mah & Song (2010a), conducted a 2-part study using 3-D body scanning to characterize air gaps, with emphasis on women's protective clothing and to evaluate predicted burn injury. In Part 1, the researchers wanted to understand how well women are protected from thermal hazards, while wearing garments designed for them, versus garments designed for men. The 3-D body scanner was used to determine the size and distribution of air gaps. Results from Part 1 showed a greater number of small air gaps versus larger air gaps. These air gaps were also not evenly spread out on the body. Part 2 focused on predicting the burn injury by using flash-fire testing. Results indicated that locations that are more susceptible to burns on the female body had either no or a smaller air gap compared to areas that had larger gaps (Mah & Song, 2010b). Body locations with no (or small) air gaps have an absence of insulating space protecting the wearer from burns.

A study by Li, Zhang, and Wang (2013) focused on establishing a quantitative relationship between air gap sizes and thermal performance. A 3-D body scanner was used for this study to measure the air gap thicknesses and volumes for 35 shirts. A thermal mannequin was used to measure the shirt thermal insulation. The results showed that the thermal insulation of the shirts increased as the air gap size also increased. However, the thermal protection actually decreased if the air gap size became larger than 1 cm (or if the volume became larger than 6000 cm^3) due to natural convection that took place because of the large air gaps.

A clothing fit study by Psikuta, Frackiewicz-Kaczmarek, Frydrych, and Rossi (2012) aimed to quantify and accurately determine the contact area and the air gap

thickness between clothing and the human body. Different garment fits (tight and loose) as well as different textile structures (woven and knit) were used. A motionless male mannequin was used for this study (Figure 2.8).

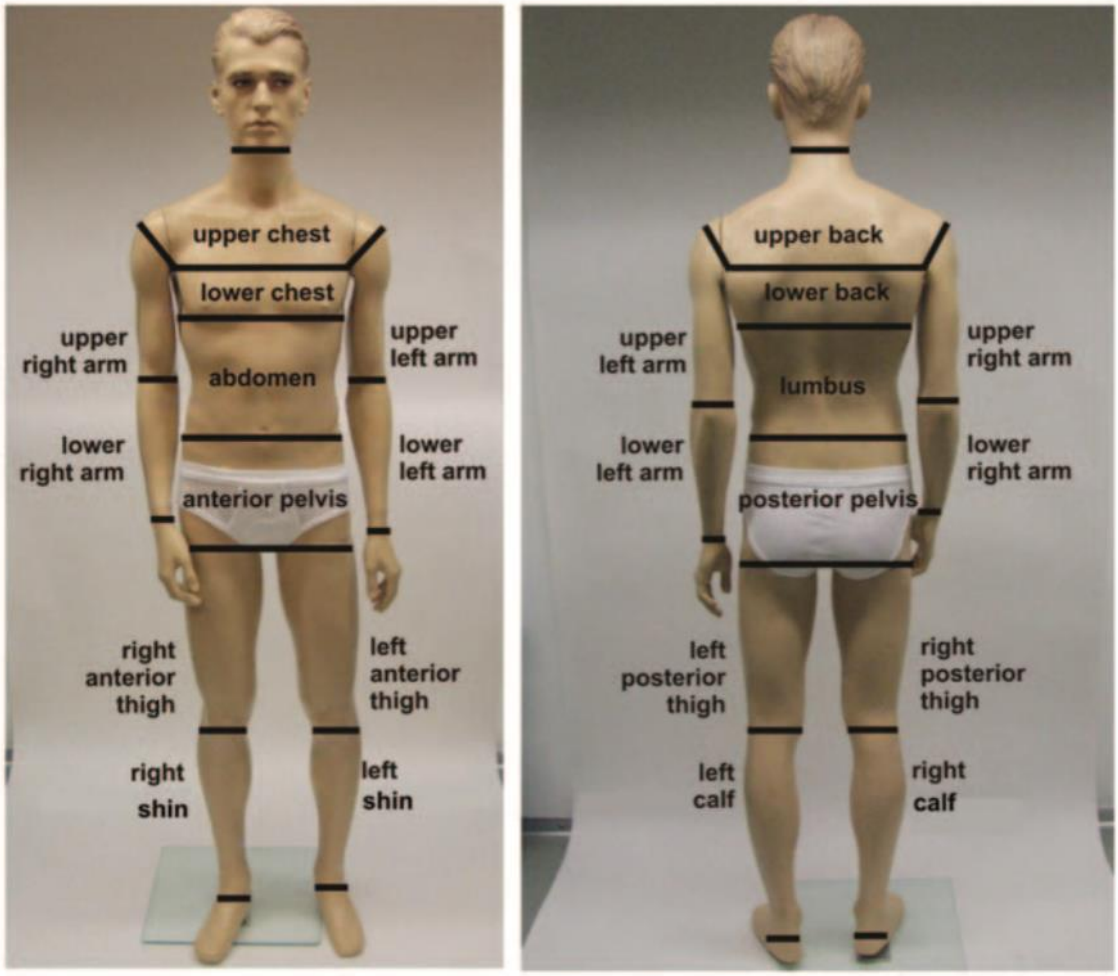

Figure 2.8: Motionless male mannequin used for study.

(Psikuta et al., 2012)

Locks were used on the mannequin to keep turning body parts in place and as a support

for the arms and feet to help keep them in a fixed position during each scan and changing scans. This is to ensure identical body positioning for all measurements. For this method, two 3-D scans using a, VITUS XXL scanner (Human Solutions GmbH, Germany), were taken (one nude and one clothed) and superimposed. Advanced 3-D scan post-processing software, Geomagic Qualify 11 (Geomagic, USA), was used to analyze the scans to obtain the required parameters: contact area and air gap thickness. Similar to previous methods addressed above, this method of measuring the body-garment relationship will work in static positions, however the subject cannot move during scanning. Therefore, this method is difficult to implement with human subjects (who are not able to precisely assume the same pose) and cannot be used when trying to evaluate the contact area or air gap thickness of a moving body.

A study by Ashdown, Loker, and Rucker (2007) investigated the fit of apparel and how it relates to existing sizing systems for specific target market populations. A mathematical model was developed to test a virtual sizing system that compares measurements from virtually created 3-D garments in relation to physically scanned 3-D measurements of a target population. This method used scans of both standing and seated posture to collect data for "active" positions. However, a limitation of this study is that the garment was not physically made or worn by a living, moving, and breathing human. This data provides general knowledge of the body-garment relationship, but does not provide data for a physical body-garment relationship, an infinite number of mobile positions, and the different variables that go along with that complexity.

These methods can be very powerful and useful, however, these methods can only

be used while the subject or mannequin is in a static position. A method of measuring the dynamic relationships is needed.

2.5.2 Force Sensing

Another approach to understanding the relationship between a garment and the body, involves force sensing. This method specifically focuses on the pressure/forces that clothing can have on the body.

A study by Zhou, Cheng, Sundholm, and Lukowicz (2014), designed a large scale textile pressure matrix sensor implemented in a variety of applications from smart clothing to household items. A smart table cloth was developed to detect different types of objects and their weight changes as content is consumed. The results show a clear difference in the signals of a glass being half full and empty. This difference was also evident in other types of dining objects, such as plates, bowls, etc. The method was also implemented in a clothing application for activity recognition and detecting movement of body parts. The smart table cloth was wrapped around the upper and lower arm and data were collected during arm movements. The results from this test showed a significant difference in the sensor signal for straight and flexed elbow. Similarly, this method was also used to test different sitting positions and a significant difference in the response signal was still present.

A study by Wong, Li, and Zhang (2004) investigated clothing pressure distributions of three sets of tight-fitting sportswear. The major focus was on the mechanical properties of the fabric of a garment and how it affected pressure in various locations on the body. Clothing pressure distributions of the three sets of tight-fitting sportswear were simulated,

as well as worn on a human body, and were compared graphically. Results showed that pressure distribution was not uniform and pressure increased significantly around the waist girth. A subjective pressure comfort rating was correlated with the simulation, showing this method can provide reliable results for pressure comfort. It was suggested that simulation would help satisfy customers' perception of comfort of a garment in terms of pressure. However, in this study the simulation and analysis were both conducted in static positions.

Tekscan® is a company that provides tactile force and pressure sensing solutions for a variety of applications. One includes understanding the amount of pressure or force applied to parts of the body. The pressure mapping system provides data through measuring and analyzing interface pressure between two surfaces. A similar product, the FlexiForce sensors, are used to measure load and force between two surfaces ("Tekscan | Pressure Mapping, Force Measurement, & Tactile Sensors," 2016). These products have been widely used in footwear studies to gain a better understanding of the forces applied to a foot (Rose, Feiwell, & Cracchiolo, 1992). Although these sensors have proven useful, according to a study that investigated the reliability of Tekscan's 5051 sensor, the system may not be able to accurately measure contact areas of joints and range of applied forces (Drewniak, Crisco, Spenciner, & Fleming, 2007). This study suggests that sensor selection plays a crucial role in the accuracy of the measurement, and that pressures close to or above the sensor's P_{sat} (saturation pressure) as well as joint areas, should be avoided.

Because of the extreme variability in clothing fit the forces applied by clothing on

the body vary considerably between bodies and over time. In addition, the body's surface has complex geometry, resulting in localized pressure points as well as distributed forces. Thus clothing moves and fits differently in different locations on the body; a challenge for some kinds of sensing. There is lack of research on how reliable various sensing approaches are in apparel or soft-good items and if the forces measured are also reflective of contact or noncontact of a garment. Cost and availability are also factors that may play a role in using these products for garment systems, especially for more reliable/accurate and/or conformable sensing systems.

A method to measure body-garment relationship in relation to contact, while mobile, would provide valuable information and data for the evaluation of fit, comfort, and mobility in a wide variety of functional garments, as well as for the purposes of evaluating LCG/LCVG cooling effectiveness. The method developed in this study has the potential of providing a new way of understanding the complexities of the body-garment relationship. It is minimally invasive, inexpensive, easy to implement and understand, and has the ability to measure both static and dynamic positions. The method also circumvents the errors inherent in other methods (such as superimposing more than one 3-D body scan), as well as the expense of sensing systems that have not been well studied in complex applications like measuring body-garment contact.

CHAPTER 3: METHOD

For this thesis, a method to measure the body-garment relationship has been developed, specifically focusing on measuring periods of contact and non-contact, while the body is mobile. This method has been developed with the intent to better understand the LCG/LCVG and body interaction; and to ultimately influence redesign and improvement of the LCG/LCVG.

The body has been used to complete a circuit with the garment, using a microcontroller and conductive materials. The method detects if a garment is in contact with the body or not. It is based on the principle of creating an electrical circuit bridging the body and the garment, and capturing a "signal" representing body-garment contact. To create the captured signal, contact of a conductive patch on the garment with the grounded body completes a circuit, allowing current to flow to the analog input of a microcontroller. It is designed to provide data about the body-garment relationship, and more specifically, to measure whether the garment is in contact with the body or not and when. A diagram of the electrical circuit used for this method is illustrated below (see Figure 3.1).

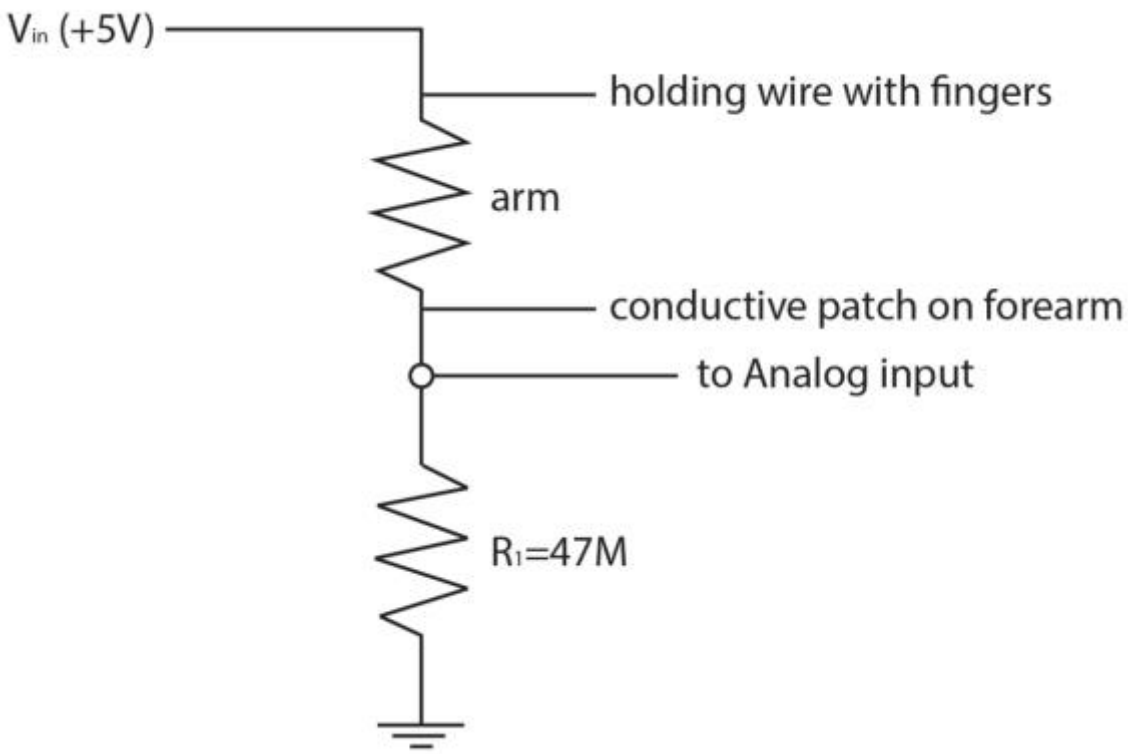

Figure 3.1: Voltage divider schematic.

This method was designed to be used in evaluating a LCG provided by NASA's Johnson Space Center (JSC) to locate and measure factors contributing to this identified body-garment contact issue. It is important to determine where these problematic areas are, as it will help in refining the problem, so solutions can be determined. This method was implemented in a pilot evaluation of the LCG to prove the concept of using this system in a dynamic garment fit evaluation. Results are presented in Chapter 6.

3.1 Apparatus Design and Construction

The apparatus designed and created for this method uses a variety of conductive materials, including thread/yarn, fabric, gel, and insulated wires, an Arduino Uno

microcontroller platform, and other standard hardware and software used for programming with microcontrollers.

The Arduino Uno is used to measure and transmit voltage readings corresponding to body contact in the garment system. A voltage-divider circuit translates resistance of the body into a voltage input on the analog pin. A 47megaohm (MΩ) resistor is used as the second half of the voltage divider, to roughly match body resistance. The voltage values read from the Arduino input fluctuate when the "switch" (contact with the body) is open or closed. When the circuit or "switch" is open (ground and analog pin are not connected), the input pin reads a very low voltage reading, close to 0Volts (V) (minimum voltage in the system). When the circuit is closed (creating a connection between ground and analog pin) the input pin reads a high voltage reading, close to 5V (maximum voltage in the system). By nature of the designed experiment, the lowest voltage reading possible is 0V and the highest is 5V.

The Arduino Uno is connected to a conductive patch by an insulated wire and an alligator clip. Insulated wires are used to connect the breadboard to the Arduino. Figure 3.2 shows the system configuration, which uses only one of the Arduino analog pins, and is designed to be used for testing one type of material or sensor placement.

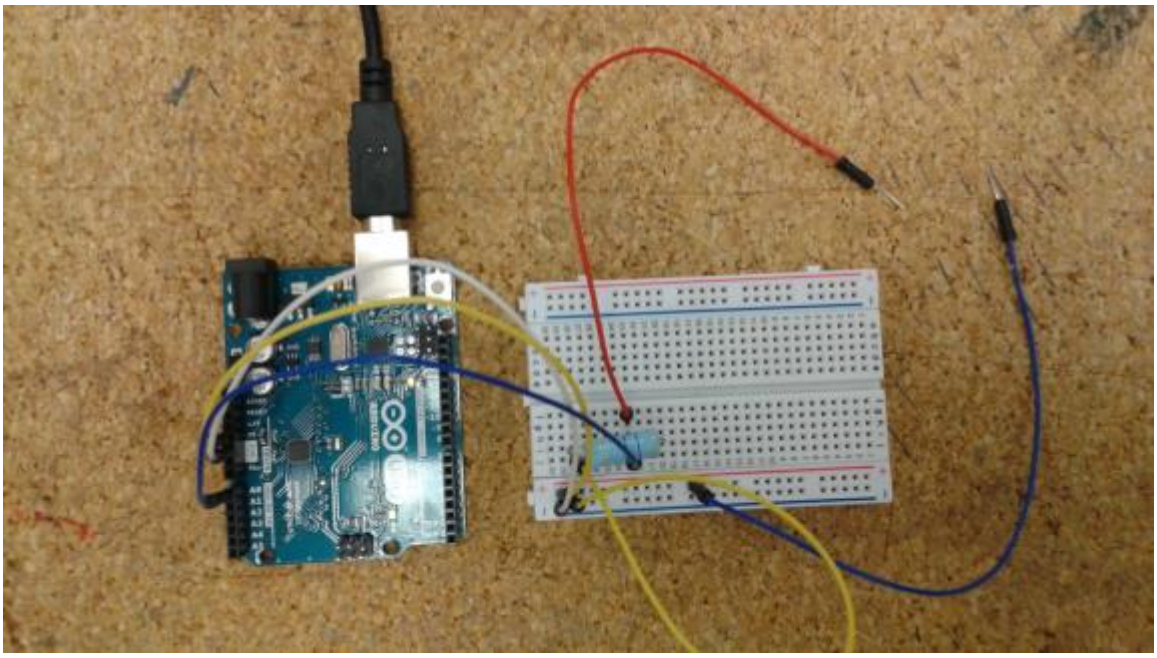

Figure 3.2: Arduino configuration for using one analog pin.

3.2 Experimental Variables

Using the method described above, three main independent variables were evaluated for effect on this system: conductive materials, weight of conductive patch, and size of conductive patch. The first variable evaluated was how different conductive materials respond to this system. A total of eight conductive materials from Less EMF, Inc. were tested. Next, the second variable tested was differing amounts of contact force applied. These tests were performed to understand how and if the amount of force that is applied between the conductive patch and the body has an effect on this system. Lastly, the third variable tested was the diameter of the conductive patch size. These tests were conducted to determine what the smallest size conductive patch could be while still proving to be effective in this system.

3.2.1 Conductive Materials

To develop this method, various conductive materials were tested to evaluate the consistency of the electrical connection created with the body, as not all conductive materials are alike. Each conductive material responds differently because conductive materials have many variables that affect the electrical connection between the material and the body. For example, conductive materials with a higher resistivity will not allow as much current to flow as materials with lower resistivity. Different conductive materials are inherently more conductive or less conductive, thus yielding different responses.

Another variable that affects electrical contact is the proportion of conductive content within a compound material, like a textile. If a material contains a relatively small proportion of conductive content, it is unlikely that it will create as strong an electrical connection with the body as a material that has a higher proportion of conductive content and therefore makes electrical contact with a larger and more continuous surface area.

Other variables that affect the way a conductive material responds to this system have to do with the surface texture of the fiber and the textile structure. Similar to "traditional" nonconductive materials, textile structure and fiber content of a textile provide a variety of different surface textures. For example, a 100% silk satin-weave textile is very smooth in texture as a result of both the fiber shape and the textile weave structure. The surface texture of a material affects the amount of contact that it may have with the body. A material that is very smooth may have a greater surface contact area with the body as opposed to a material that is highly textured, due to parts of the texture folding away from the body. On the other hand, a highly textured material may provide a more localized contact force against the body. So, even though it may not have as large of

a surface contact area, the amount of force that it is placing on the body is greater because of the geometry of the material.

The "Fabric Sampler Booklet" from Less EMF, Inc. (Less EMF Inc., Latham, NY, www.lessemf.com), which contains eight different types of conductive materials was used. Each of these conductive materials were evaluated to gain a deeper understanding of how each material responds to this system.

The known properties of the materials used in this experiment are summarized in Table 1.

Table 1: Conductive material properties.

Material	**Structure**	**Fiber Content**	**Resistivity**	**Stretch Direction**	**Stretch %**	**Notes**
#1 Conductive stretch fabric	Knit	Medical grade silver-plated 92% nylon, 8% Dorlastan	Surface resistivity of <1 Ohm/square(sq.)	lengthwise and crosswise (4-way-stretch)	N/A	This is a highly conductive material and decreases in conductivity as it stretches
#2 Copper FlecTron	Woven (ripstop weave)	100% nylon	surface resitivity of <0.1 Ohm/sq.	N/A	N/A	Subjected to an electroless copper plating process
#3 Nickel Mesh	Woven (loose weave)	Polyester-core fibers	Surface resistivity of <0.1 Ohm/sq.	N/A	N/A	Coated with copper and then nickel
#4 Silver Mesh	Knit	Silver-coated nylon fibers	Electrical resistance of <0.5 Ohm/sq.	Lengthwise (little to no stretch in the crosswise direction)	50%	N/A

#5 VeilShield	Woven	Polyester fibers (coated with zinc-blackened nickel over copper)	Resistivity of 0.1 Ohm/sq.	N/A	N/A	N/A
#6 EX-STATIC	Knit	87% polyester, 13% BASF Resistat (carbon) (woven directly into the textile in a diamond pattern)	Surface resistivity of 10^5 Ohm/sq.	Crosswise	16.67%	Conductive elements only concentrated in the small diamond pattern. No elastomeric fiber content, this textile has very little stretch
#7 Hook-side fastener	Nonwoven with molded hooks	N/A	1.8 Ohm/sq.	N/A	N/A	Silver coated
#8 Loop-side fastener	Nonwoven with molded loops	N/A	1.4 Ohm/sq.	N/A	N/A	Silver coated

Eight different types of conductive materials were investigated for their potential use to be implemented in this method of measuring body-garment contact. Material #1-#6 are textiles and Material #7 and #8 are fasteners, more commonly known as Velcro™. A 100% cotton knit textile was used as the backing onto which conductive patches of various materials were attached to for testing the contact method. The size of each conductive textile (Material #1-#6) was 3.81 cm in diameter, and the size of the hook and

loop fastener (Material #7 and #8), were both 3.81 cm in length (see Figure 3.3). The conductive patch for each material was taped securely onto the textile using transparent adhesive tape.

Figure 3.3: Conductive materials tested.

In Material #6 (EX-STATIC Conductive Fabric), the conductive elements are concentrated in a small diamond pattern, creating a textile with a relatively low proportion of conductive material in relation to the other materials tested. Because it has no elastomeric fiber content, this textile has very little stretch. However, its knit structure inherently imparts some stretch.

The fastener material used in #7 (Conductive Hook Fastener) and #8 (Conductive Loop Fastener) have both a "hook" and a "loop" side, that when touched together, "fasten" like Velcro™. The hook side of this material is stiffer and scratchier than the loop side. The loop side of this fastener is much softer and fuzzier than the hook side. Because this material is a nonwoven structure, it has no inherent stretch qualities.

3.2.2 Contact Force

After tabletop testing of the eight conductive materials was complete the data were analyzed. The conductive hook fastener created the strongest electrical contact with the body and was selected for further tests. A contact force test was conducted to determine if the material responded with a different connection voltage when different amounts of contact force were applied between the patch and the body. A variable response could mean that this method could be used to measure force, in addition to measuring body-garment contact. To roughly understand how force affects this system and the sensor, two conditions were tested that have very different contact forces. In the first condition the weight of one human arm (resting on top of the conductive patch) was used to apply force to the conductive patch. In the second condition only the weight of the small conductive patch (resting on top of the human arm) was used to apply force to the body.

3.2.3 Patch Size

To understand in more depth how the selected material for this method responds in different physical configurations, circular conductive patches of various diameters were tested next. It is valuable to know how small the diameter of the conductive patch can be, while still enabling effective detection of body contact. Though the conductive patches tested in the earlier tests were relatively small (3.81 cm) and unlikely to cause interference with the garment and the wearer, the ability to implement the smallest possible conductive patch in the garment would provide the least amount of interference and improve the granularity of measurement over a garment area.

To minimize the patch size for garment integration, different patch diameters were

tested to determine the smallest possible patch size that could be viable for detecting body-garment contact in this system. Five different sized circular patches were created using the conductive hook fastener. The patch diameters tested were: 2.54 cm, 1.905 cm, 1.27 cm, 0.635 cm, and 0.3175 cm (Figure 3.4).

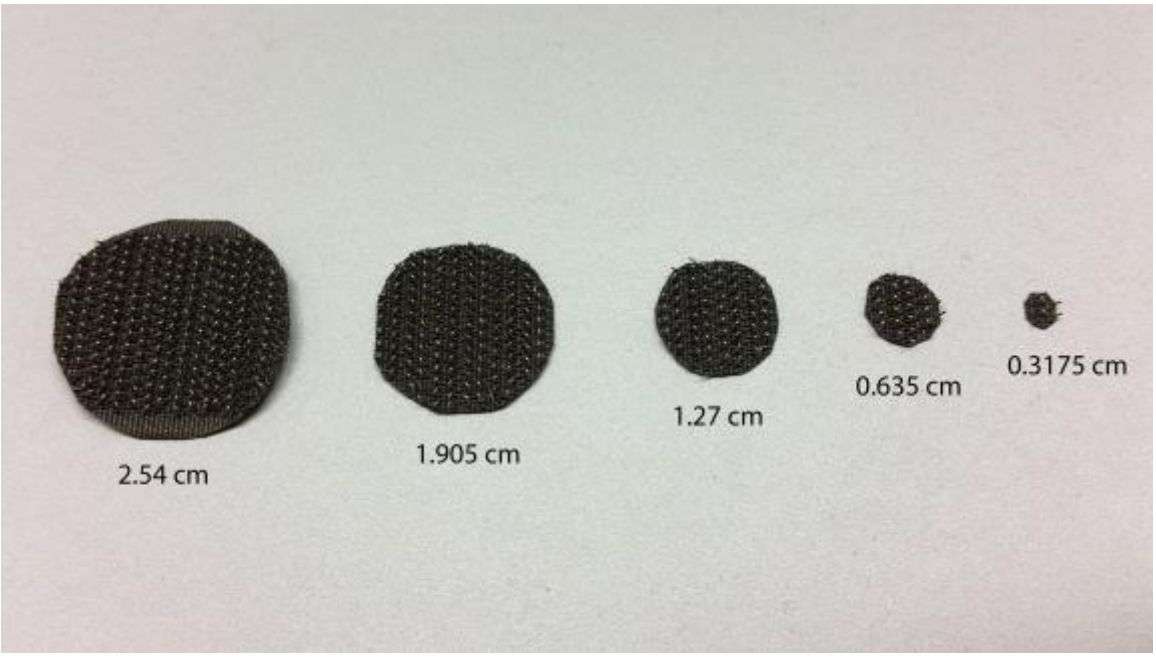

Figure 3.4: Conductive patch sizes.

3.3 Method: Material Evaluation

3.3.1 Test Procedure: Conductive Materials

Each conductive material evaluated was laid on a flat table surface. The analog pin from the Arduino was connected to the conductive patch using an alligator clip. A small portion of the edge of the conductive patch was purposefully draped over the side of a table surface to eliminate any potential alligator clip interference in the surface contact of the body with the conductive patch.

Connection with the human body of the wear tester was made through the wire from the VCC pin (+5 V) of the Arduino by firmly grasping it in the wear tester's left hand between the index finger and thumb. Contact was maintained throughout the entirety of each trial. In order to allow for the greatest amount of connection, conductive gel was applied to the index finger and thumb prior to each trial.

The same female wear tester was used for all tests in this study.

For each material, a timed 1-minute trial was performed. Each 1-minute trial consisted of timed 5-second intervals of deliberate, alternating contact and noncontact, starting with noncontact and ending with contact. A timer was used to control the 5-second intervals and the 1-minute trial.

To test for noncontact, the wear tester's arm holding the ground wire was raised above and away from the conductive patch, creating a gap between the conductive patch and the arm (see Figure 3.5). This procedure is meant to simulate a garment not being in contact with the body and having an air gap, which in this system, opens and breaks the loop of the circuit created.

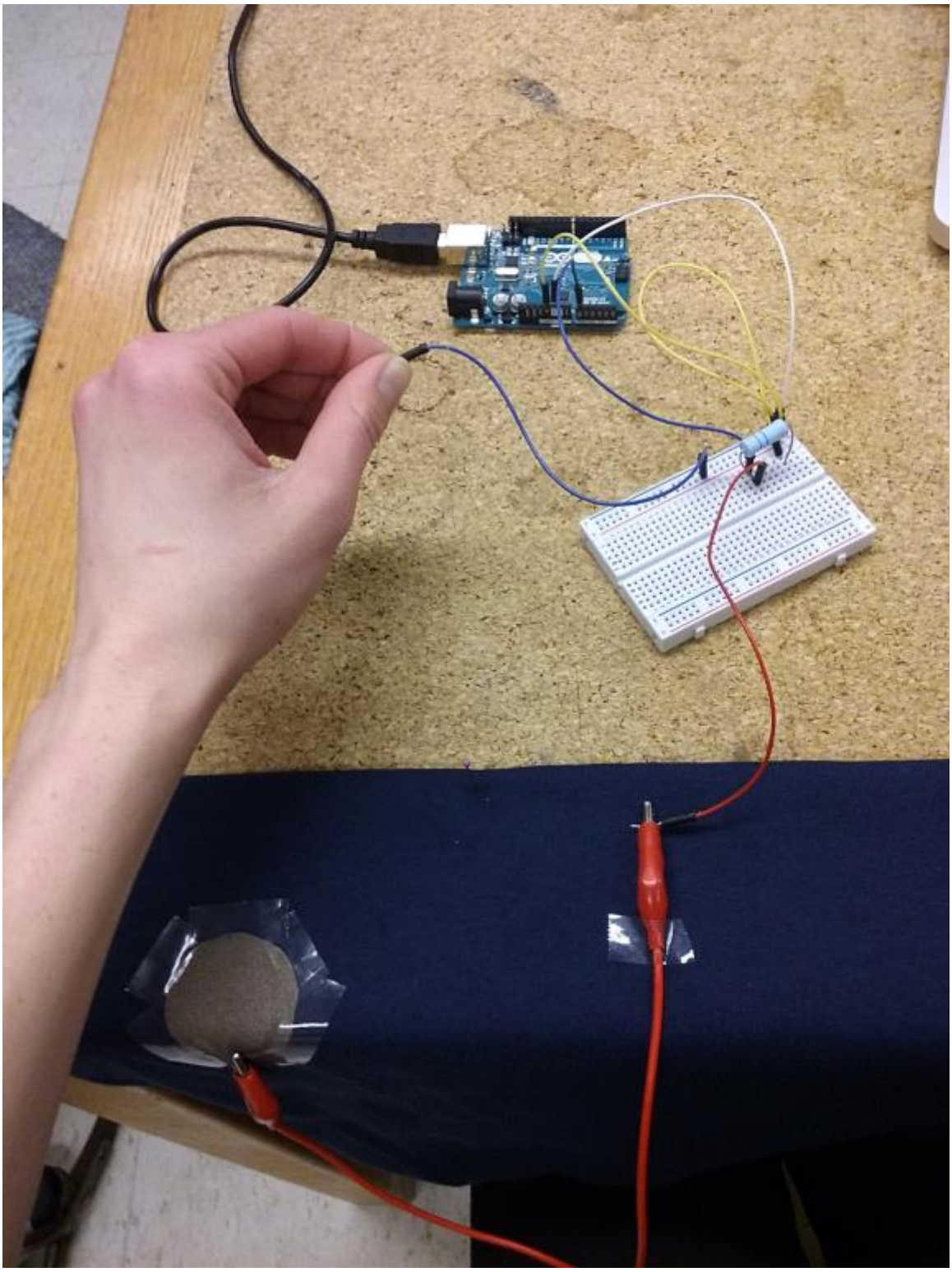

Figure 3.5: Testing noncontact.

To test for contact, the arm holding the ground wire was lowered and pressed with light force against the conductive patch on the table surface, creating contact between the conductive patch and the arm (see Figure 3.6). This procedure is meant to simulate a garment touching and being in contact with the body, which in this system, closes the loop of the circuit.

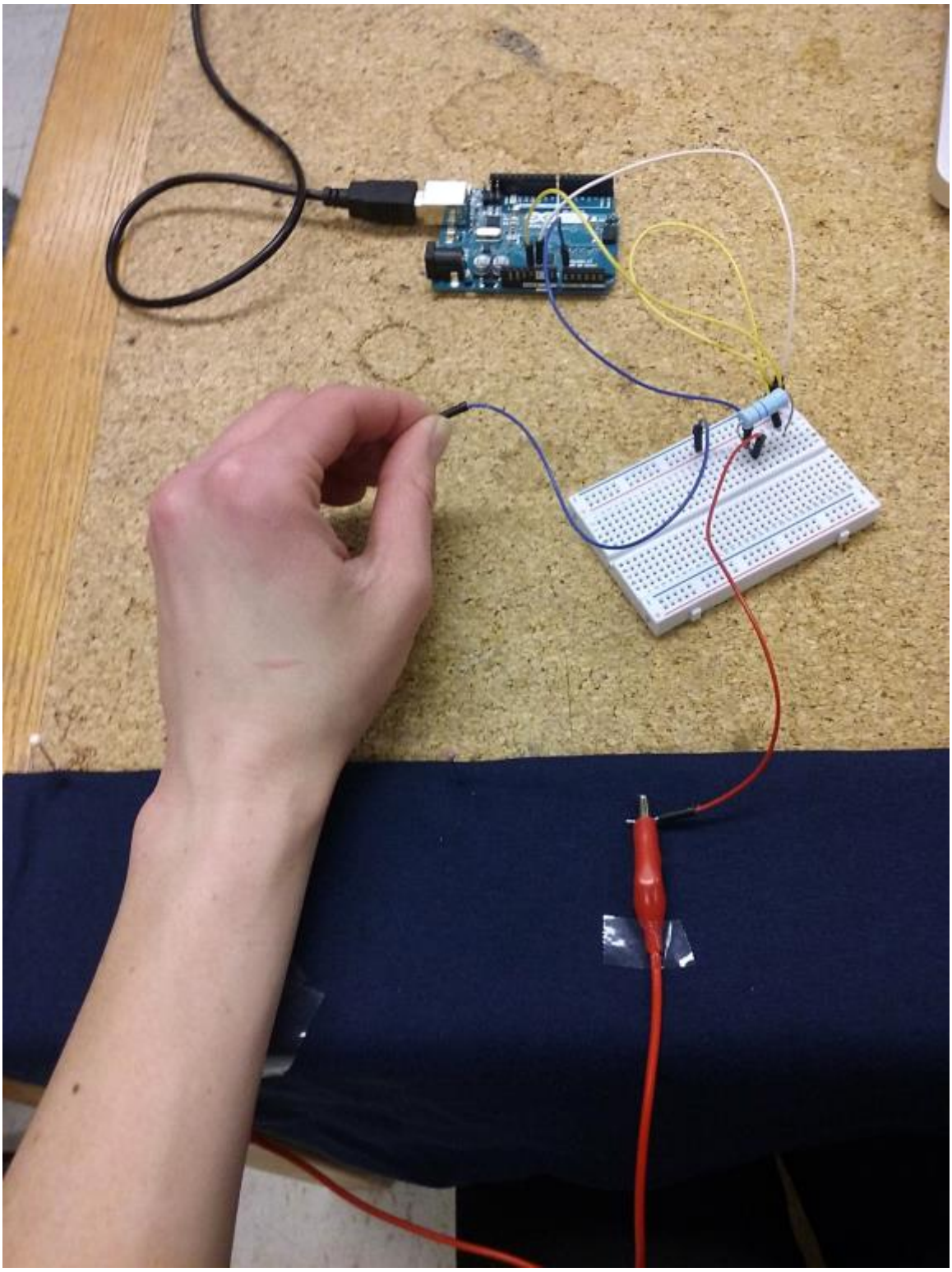

Figure 3.6: Testing contact.

The arm was applied to the material with some amount of force greater than arm weight. Although the same wear tester performed all trials and aimed for consistency in the amount of force applied, this was not controlled precisely.

The data collected from the Arduino board were recorded for processing and analyzing using CoolTerm™, which is a simple serial port terminal application ("Roger Meier's Freeware," 2016).

The voltage readings from the analog input pin were recorded at 10Hz by the Arduino platform, through the serial interface. A reference measure representing the test procedure was manually reconstructed, consisting of alternating 5-second intervals of 0V and 5V.

3.3.2 Data Analysis: Conductive Materials

The data from the Arduino board was recorded using CoolTerm™ and saved as a text file for each trial. The text files were imported into separate Microsoft Excel files for further analysis.

Line graphs were created for each of the eight conductive materials. Stimulus reference values were manually reconstructed for each trial based on the timing of the test, as alternating 5-second periods of 0V ("noncontact") to 5V ("contact"), according to the timing of the test. The Arduino voltage value and the reference stimulus were graphed together for visual analysis of the data.

A simple linear regression was performed to calculate the r-squared value for each material, which was used as a coarse quantitative measure reflecting the correlation

between the recorded voltage signal and the reference stimulus.

3.3.3 Test Procedure: Contact Force

The same procedure used to test the eight conductive materials with slight variations was used to test contact force. Each trial was approximately 1-minute in length, with alternating 5-second intervals of deliberate contact and noncontact, starting with noncontact and ending with contact. However, the way in which contact between the arm and the conductive patch was created differed for these two trials.

In order to test body weight contact force, the conductive patch was placed on the surface of a flat table top (as it was for testing of the eight conductive materials) and the arm was raised above the conductive patch (to create noncontact) and lowered onto the surface of the conductive patch (to create contact), in 5-second intervals.

To compare the contact force of the patch weight, the arm and the conductive patch switched positions. During this trial the arm remained resting on the flat table surface (where the conductive patch previously was), while the conductive patch was raised away from the arm (to create noncontact) and lowered gently to be placed on top of the arm (to create contact), in 5-second intervals. During this trial careful attention was paid to preventing accidental electrical interference by creating an unintentional connection with the hand that was used to lift and lower the conductive patch onto the test arm. Insulation for conductive elements was used and the hand was kept as far away as possible from the connection between the alligator clip and the conductive patch.

3.3.4 Data Analysis: Contact Force

The analysis of patch and arm weight data was the same as the analysis for various conductive materials data, mentioned above. Each trial was approximately 1-minute in length, with alternating 5-second intervals of deliberate contact and noncontact, starting with noncontact and ending with contact. Line graphs with a manually added reference stimulus were created for visual analysis of voltage values for both trials.

3.3.5 Test Procedure: Patch Size

The same method with few alterations used in previous trials was used to test various patch sizes. The same apparatus and method of testing (tabletop) was used for testing patch sizes. However, instead of alternating between 5-seconds of intentional contact and noncontact, contact was maintained between the arm and the conductive patch for the entirety of a 1-minute trial for each patch size, to measure an average voltage value for each patch size.

3.3.6 Data Analysis: Patch Size

The data recorded for various patch sizes were analyzed in a similar manner. The text file generated by CoolTerm™ from the Arduino platform was imported into Microsoft Excel for analyzing. A line graph was created for each trial for qualitative visual analysis. No stimulus reference value was manually reconstructed for these trials, due to the difference in how the data was collected (no alternating between contact and noncontact—contact was kept the entire time). A simple regression was not performed in the analysis of this data, due to the absence of a manually constructed stimulus reference

value, but rather the average voltage of each trial was calculated for analysis.

CHAPTER 4: RESULTS

4.1 Conductive Fabrics

The results for each of the eight materials are depicted in Figures 4.1-4.8, followed by the r-squared values for all of the materials tested depicted in Figure 4.9. The blue line in each line graph represents the voltage value reading of the specific material tested. The red line is a manually added stimulus for reference of alternating, timed 5-second intervals, representing contact and noncontact of body-garment (microcontroller switch closed and opened).

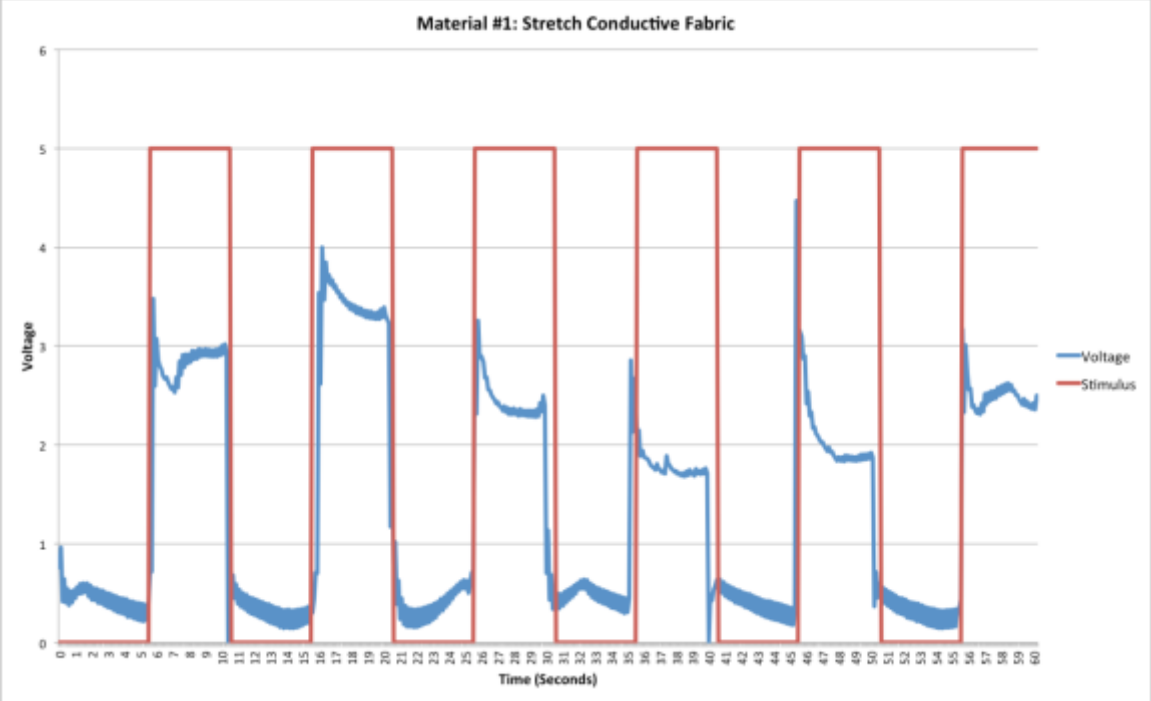

Figure 4.1: Material #1: Stretch Conductive Fabric.

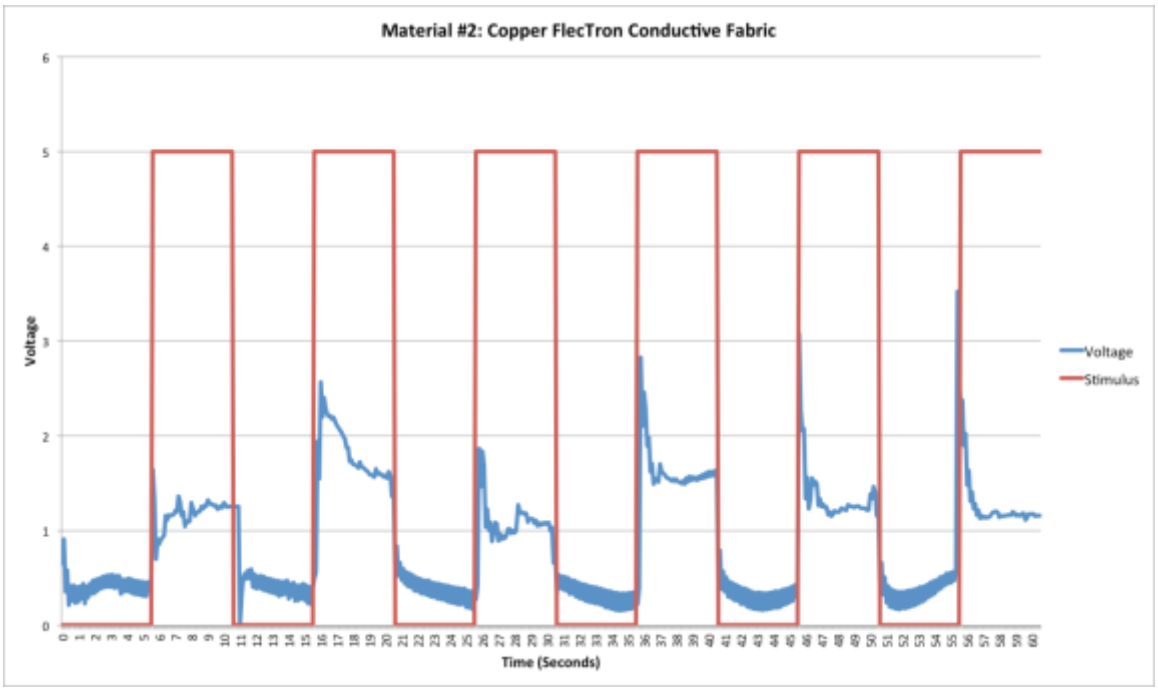

Figure 4.2: Material #2: Copper FlecTron Conductive Fabric.

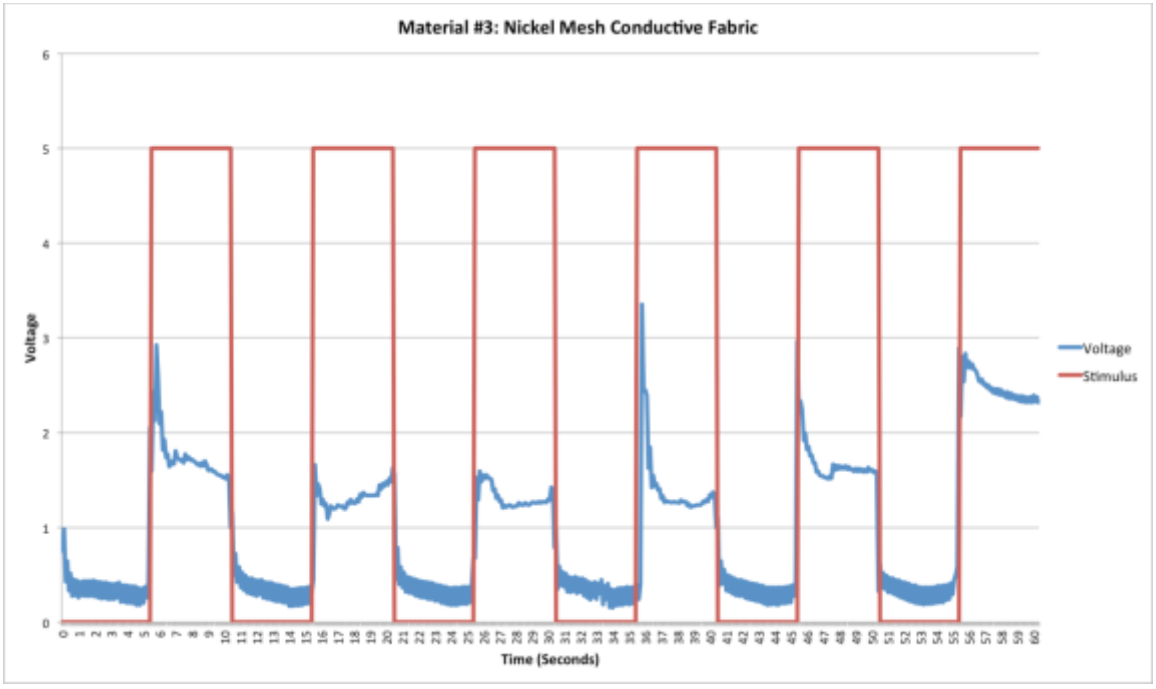

Figure 4.3: Material #3: Nickel Mesh Conductive Fabric.

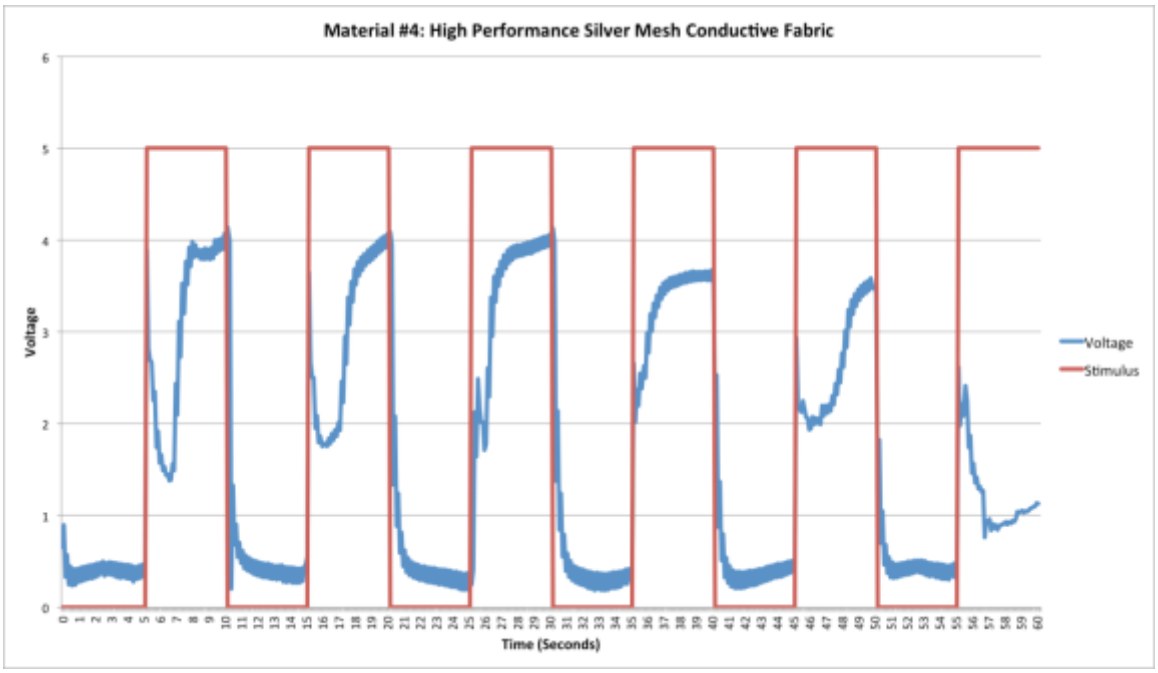

Figure 4.4: Material #4: High Performance Silver Mesh Conductive Fabric.

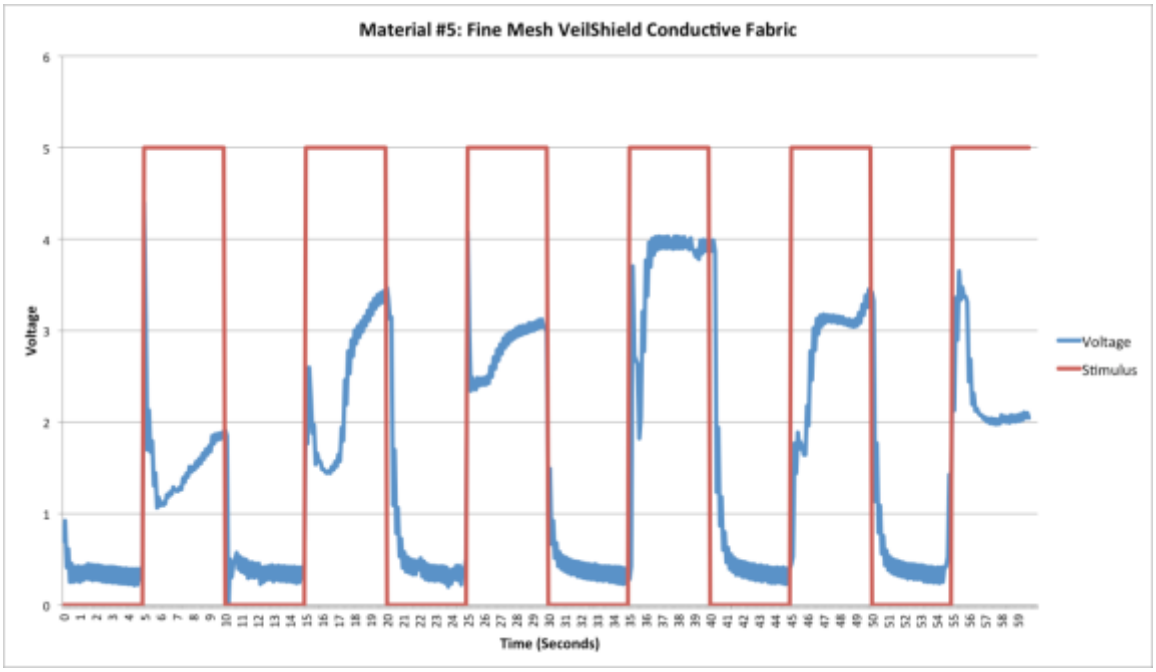

Figure 4.5: Material #5: Fine Mesh VeilShield Conductive Fabric.

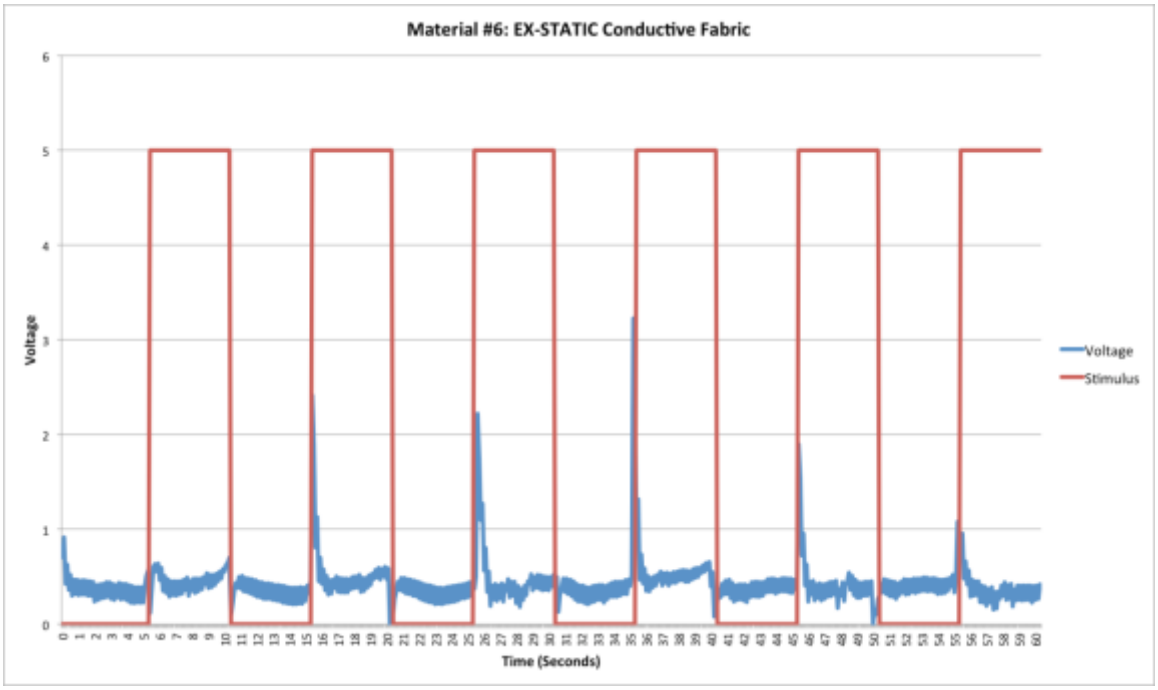

Figure 4.6: Material #6: EX-STATIC Conductive Fabric.

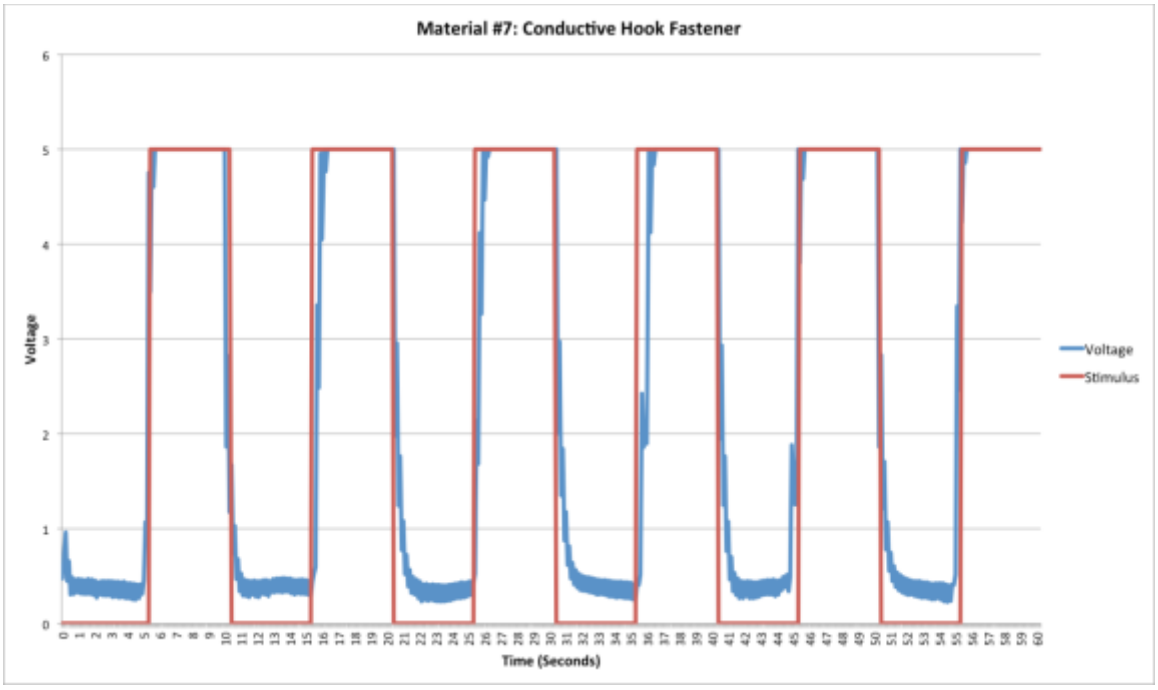

Figure 4.7: Material #7: Conductive Hook Fastener.

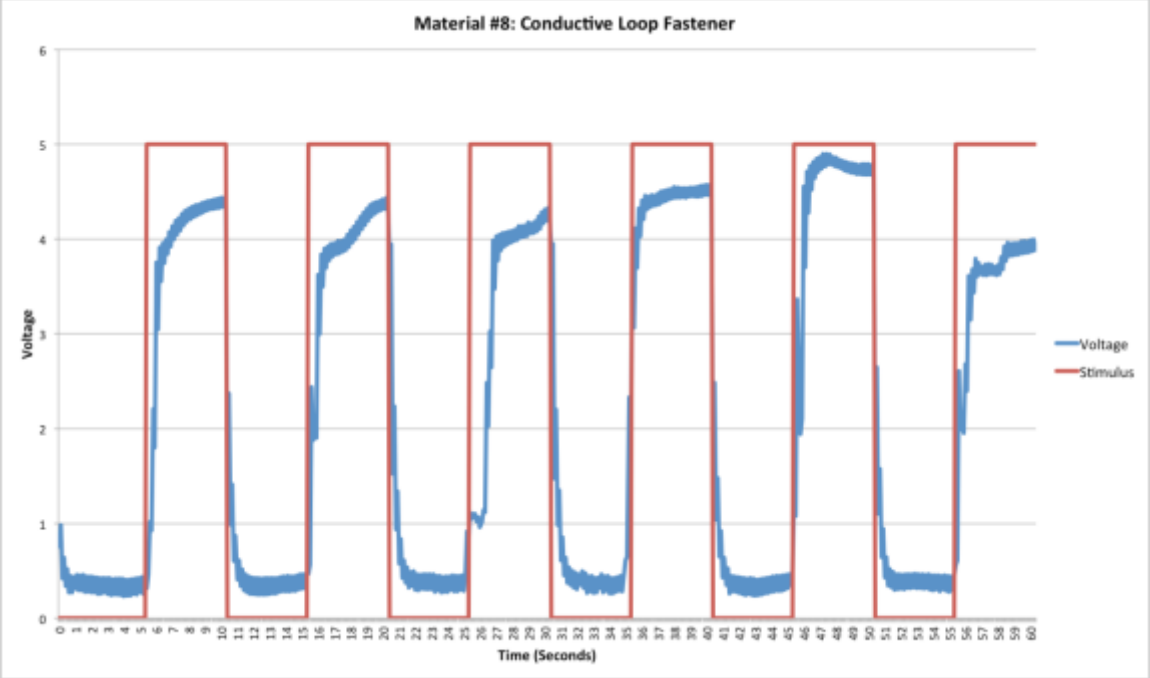

Figure 4.8: Material #8: Conductive Loop Fastener.

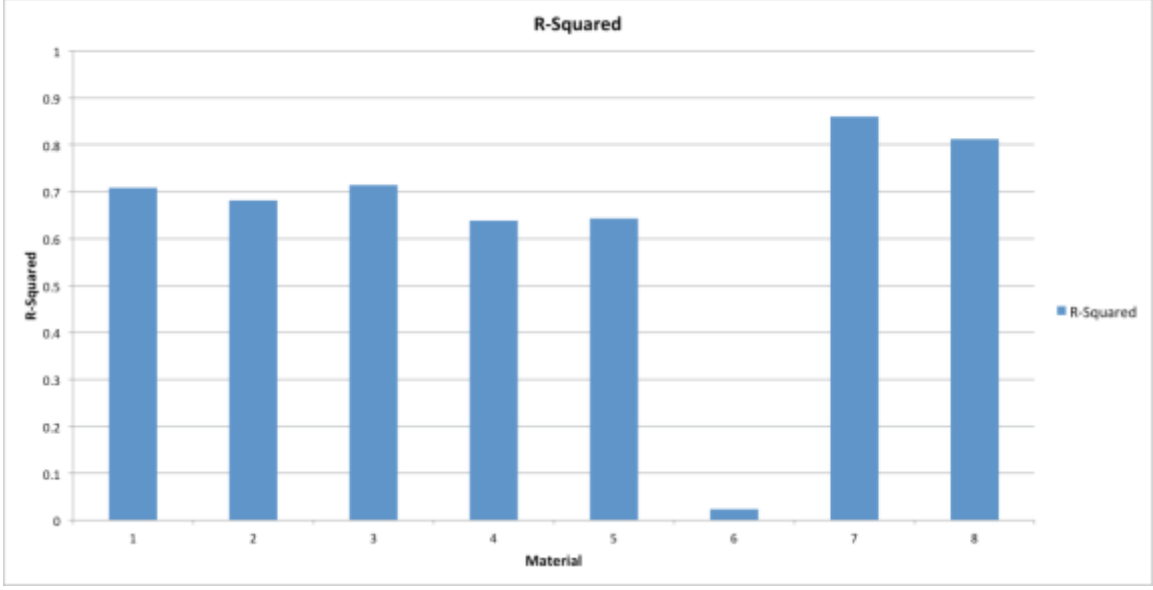

Figure 4.9: R-squared values for materials tested.

4.2 Contact Force

The results from testing contact force are depicted in Figures 4.10-4.11. Similar to the other line graphs above, the blue line in each graph represents the voltage value reading of the specific material tested. The orange line is a manually added stimulus for reference of alternating, timed 5-second intervals, representing contact and noncontact of body-garment (microcontroller switch closed and opened).

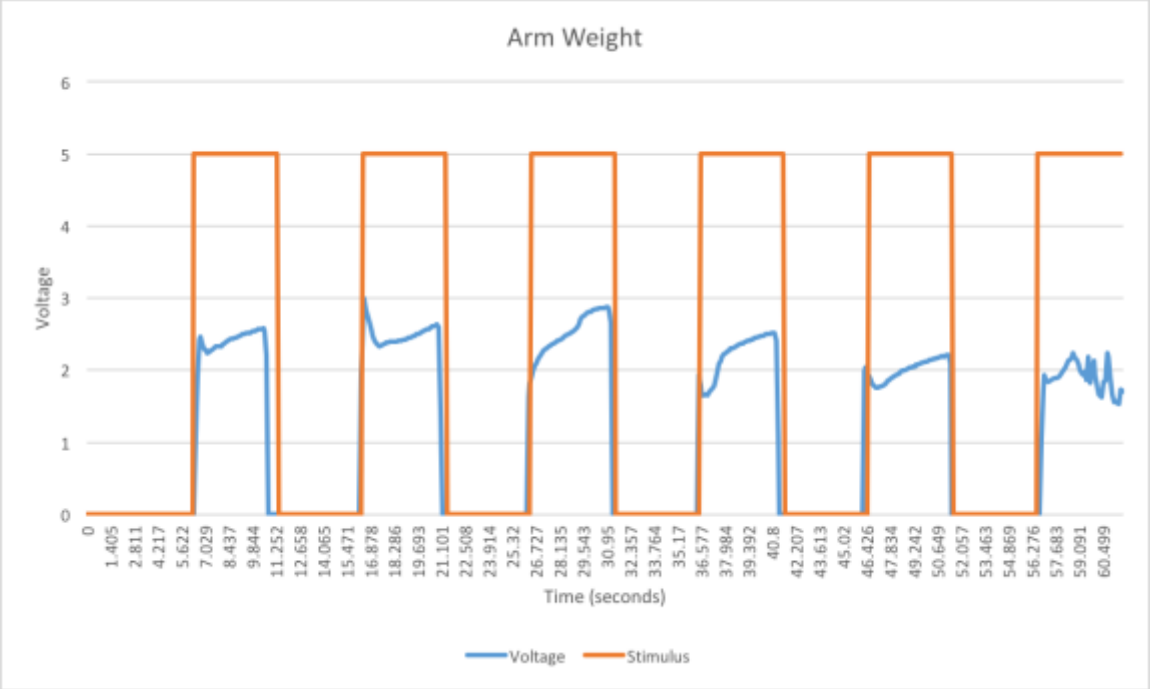

Figure 4.10: Arm weight.

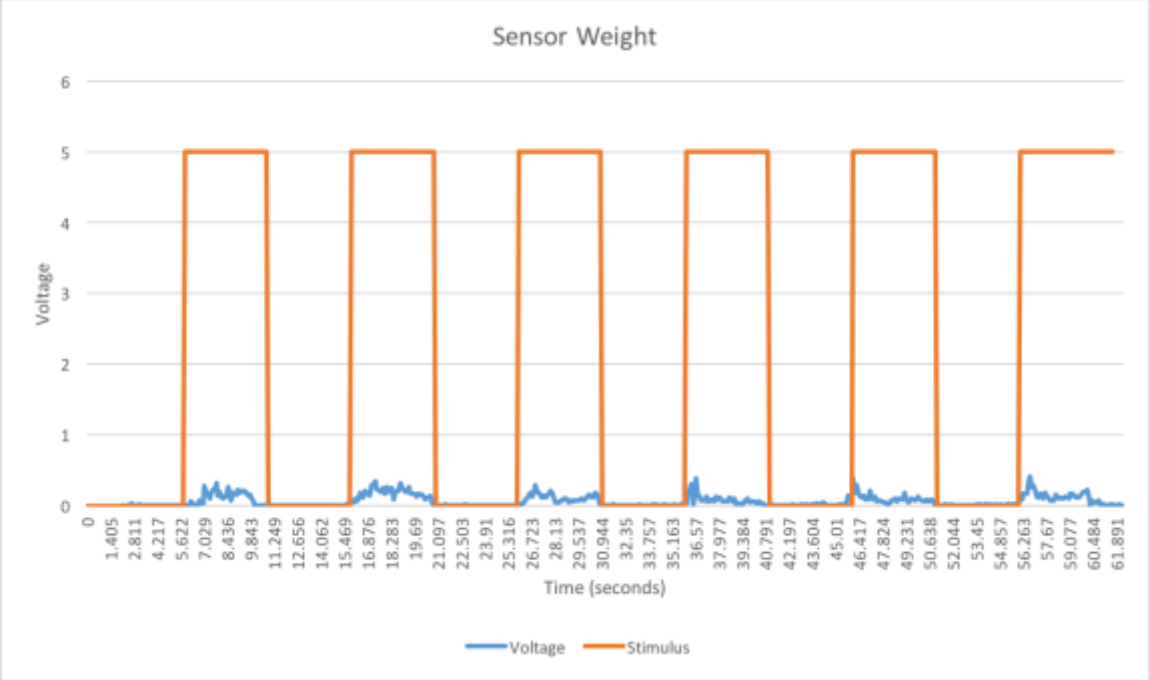

Figure 4.11: Sensor weight.

4.3 Patch Sizes

The results of the five different conductive patch size tests, are depicted in Figures 4.12-4.16. There is only one line in these graphs, as contact between the arm and the conductive patch was maintained for the duration of the trial and there was no manually constructed stimulus reference value added. The blue line in each line graph represents the voltage value reading of the specific circle hook patch size tested. A bar chart (Figure 4.17) shows the average voltage and standard deviation of each conductive patch size.

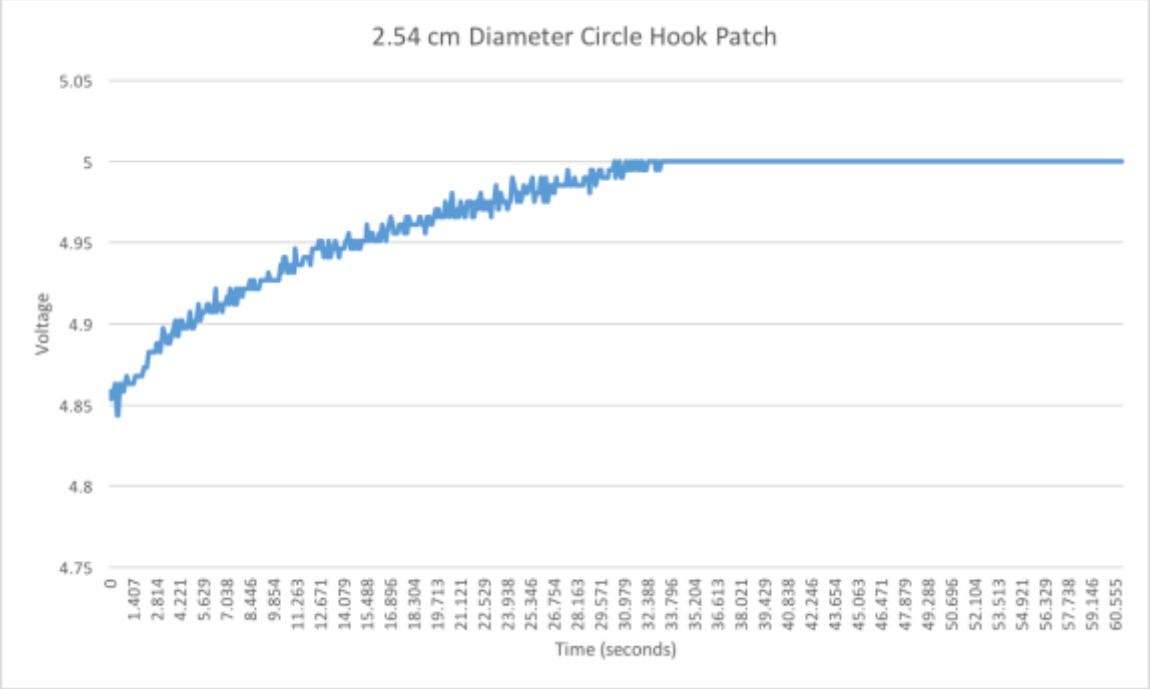

Figure 4.12: 2.54 cm Diameter circle patch.

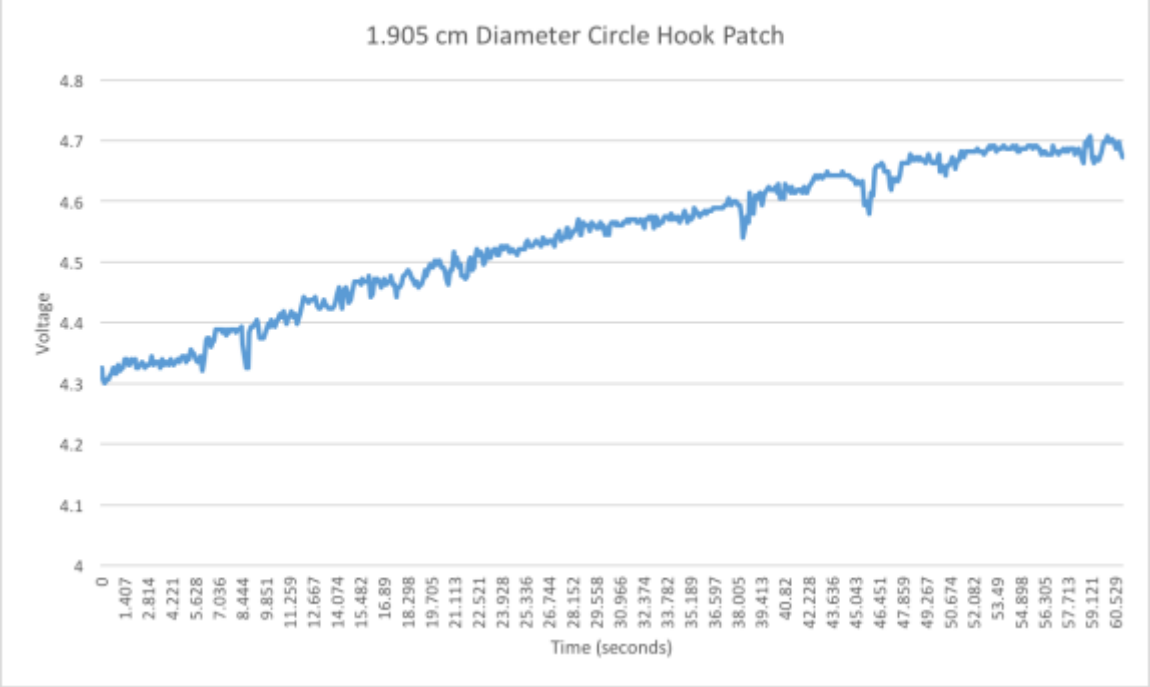

Figure 4.13: 1.905 cm Diameter circle patch.

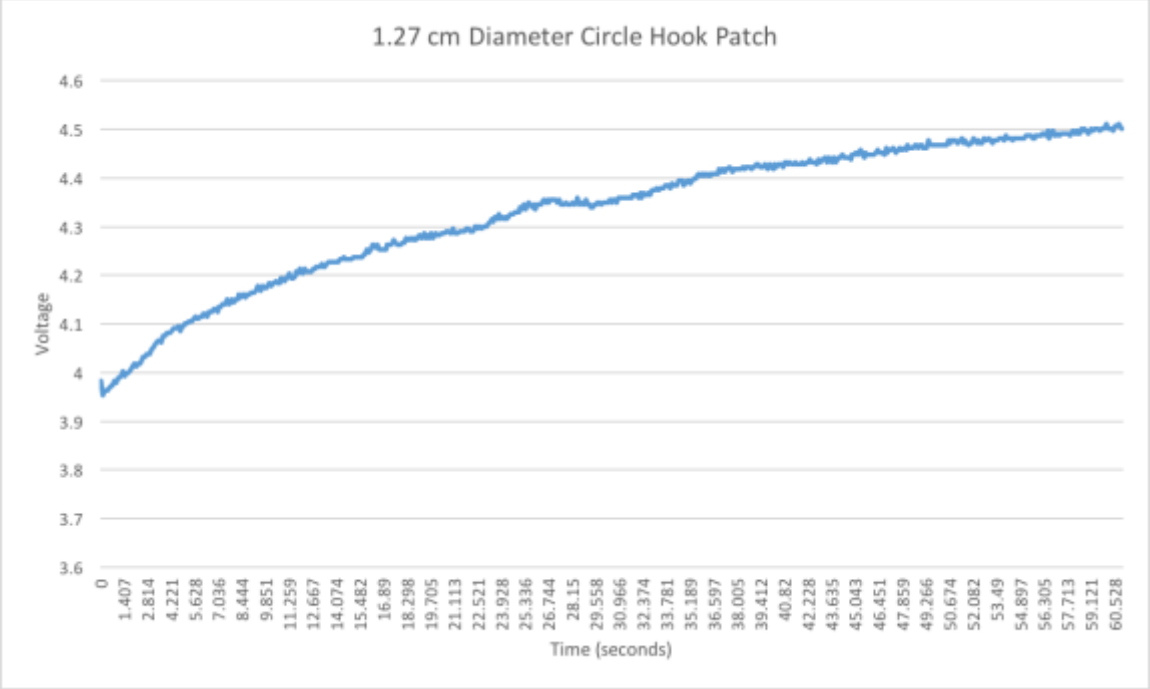

Figure 4.14: 1.27 cm Diameter circle patch.

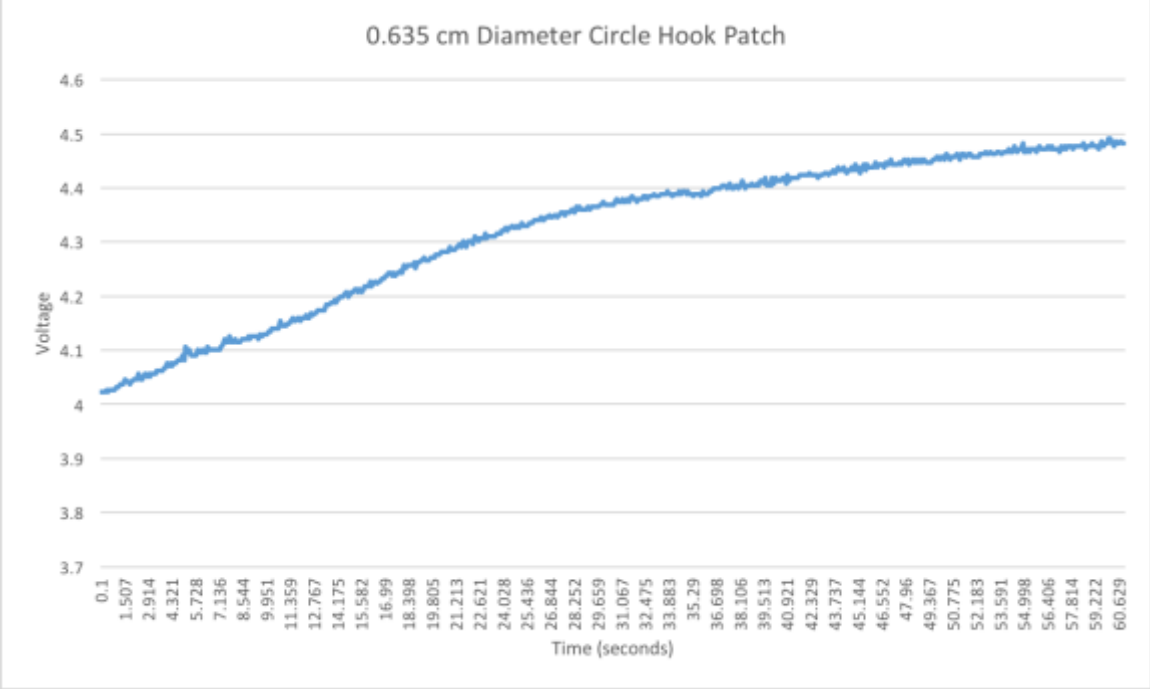

Figure 4.15: 0.635 cm Diameter circle patch.

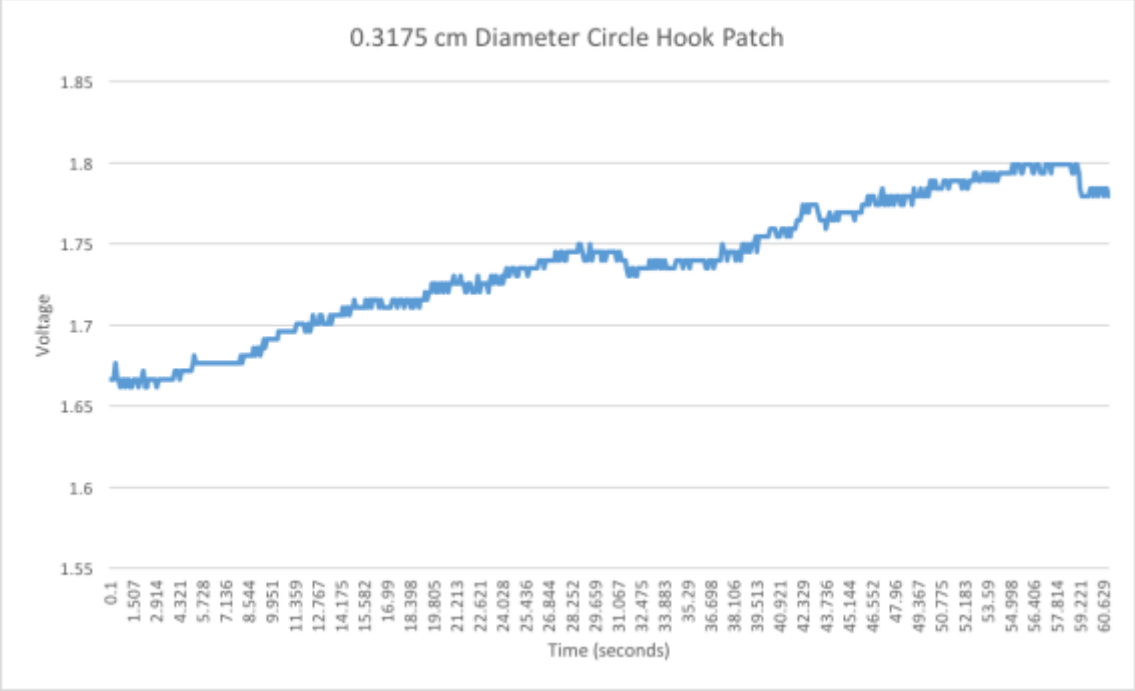

Figure 4.16: 0.3175 cm Diameter circle patch.

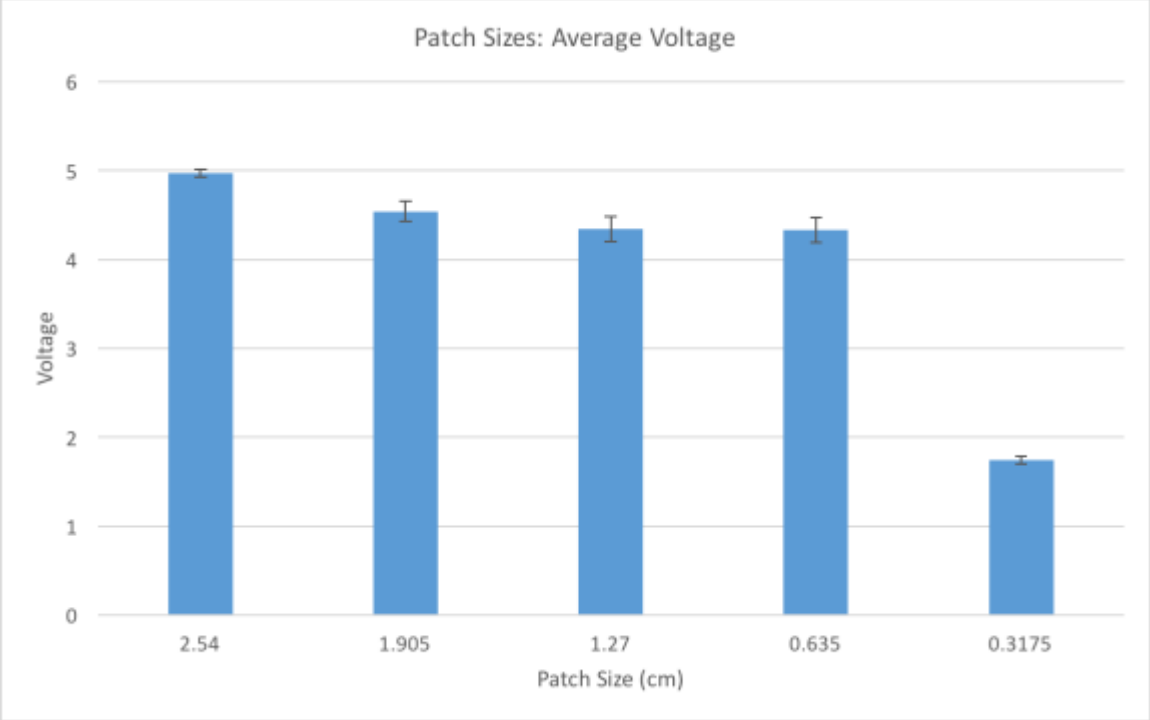

Figure 4.17: Average voltage and standard deviation

CHAPTER 5: DISCUSSION

5.1 Discussion: Conductive Materials

Seven of the eight materials tested showed a voltage response in the presence of body contact that could (in some cases with modifications to the voltage-divider circuit, and in all cases with the establishment of a cut-off threshold for determining "contact") be viable for detecting contact between body and garment. Material #6 (EX-STATIC Conductive Fabric) did not show a show a voltage response that could be viable for detecting contact.

More noise was observed in the signals recorded from Material #4 (High Performance Silver Mesh Conductive Fabric), #5 (Fine Mesh VeilShield Conductive Fabric), #6 (EX-STATIC Conductive Fabric), and #8 (Conductive Loop Fastener), and in contrast, Material #1 (Stretch Conductive Fabric), #2 (Copper FlecTron Conductive Fabric), #3 (Nickel Mesh Conductive Fabric), and #7 (Conductive Hook Fastener) provided the smoothest signal of the group, with less noise.

Material #6 (EX-STATIC Conductive Fabric) had the weakest response of all the materials tested. There was very little conductive material within this textile, which is likely to have contributed to the weak electrical response to the 5-second intervals of contact.

Material #7 (Conductive Hook Fastener) provided the smoothest signal of all the materials tested. Though Material #7 (Conductive Hook Fastener) was the stiffest material tested, in the intended application it is possible that it would be used in such a small patch that it should not have any more of an adverse effect on the LCG/LCVG than the non-pliable tubing does. (A future goal of this method is to use the smallest possible

sensor size that will still be able to detect body-garment contact.)

The r-squared values (Figure 4.9) of each material tested are used as a general measure of the correlation of each material's voltage signal and the "expected" or reference value. Material #6 (EX-STATIC Conductive Fabric) has the lowest correlation at 0.024. Material #7 (Conductive Hook Fastener) has the highest correlation at 0.861. All other materials are close to 0.7, except for Material #8 (Conductive Loop Fastener), which is close to 0.8.

The r-squared values observed in the materials that had a noisier response (Material #4 (High Performance Silver Mesh Conductive Fabric), #5 (Fine Mesh VeilShield Conductive Fabric), #6 (EX-STATIC Conductive Fabric), and #8 (Conductive Loop Fastener)) also had lower r-squared values, in comparison to the materials tested that had a much smoother and less noisy response. (In this evaluation, noise was not quantified – but is evident from a visual analysis of the graphs of each material response.) Materials #7 and #8 show a smoother and stronger response in relation to the r-squared values.

Material #7 (Conductive Hook Fastener) was chosen as the material to be tested in a garment for this method of measuring body-garment contact, due to its high r-squared value, and thus strong response to the system.

5.2 Discussion: Contact Force

The voltage value that was observed while testing arm weight was slightly above 2V. In contrast, the voltage value that was observed while testing patch weight was dramatically lower and was barely over 0V. This is most likely due to the fact that pressure has a significant effect on the system and the connection between the body and

the conductive patch. As more weight is applied between the body and the conductive patch a stronger connection is made, thus a higher voltage response value is observed.

These results show that contact force is a contributing factor in the response of the sensor and has an effect on this method. However, because only two amounts of force (relatively high and relatively low) were tested, it is not clear how linear this relationship is. Further investigation on exactly how force affects this system would be useful to know in order to determine how much it may potentially be a confounding variable, as well as to determine whether or not contact force can be actually measured using this approach.

5.3 Discussion: Patch Size

Illustrated in each of the graphs of the results from testing different patch sizes, the voltage response of each conductive patch size gradually increases incrementally as (contact) time progresses. This increase of voltage that is present in every trial is most likely due to the connection between the body and the conductive patch increasing and becoming more strong as time passes. However, the average voltage value for each patch size also varies.

The largest patch (2.54 cm diameter) tested unsurprisingly showed the highest voltage response overall to the system. This patch started off at roughly 4.85V and gradually increased to 5V (the maximum possible voltage of this system) where it topped out at and stayed for the rest of the duration of the 1-minute trial test. The average voltage for this conductive patch size is 4.97V.

The second largest conductive patch (1.905 cm diameter) showed the second highest voltage response overall. The results from this trial are similar to that of the 2.54

cm test, however, the voltage value is slightly lower (between 4.3 and 4.7 V) and does not reach or top off at 5V—the voltage value continuously increases without reaching its maximum reading. This conductive patch size had an average of 4.54V.

The next two patches (1.27 cm and 0.635 cm diameter) show very similar responses. Both of these conductive patch sensor sizes show a lower voltage response in comparison to the 1.905 cm and 2.54 cm conductive patch sensor sizes. They both have very similar voltage values, which start off at the beginning of the trial around 4V and increase to around 4.5V at the end of the trial. The 1.27 cm diameter conductive patch had an average of 4.34V and similarly the 0.635 cm diameter conductive patch had an average of 4.33V. These two conductive patch sizes performed very similar during testing.

The smallest conductive patch (0.3175 cm diameter) had a drastically different voltage response than all the other conductive patch sensor sizes tested. The voltage value for this sensor started off at around only 1.65V and increased to 1.8V at the end of the trial. The average was 1.74V. This sensor has the lowest voltage response to the system by a drastic amount and also appears to have the smallest increase in voltage for the duration of the trial. This patch is very small and because of that it does not seem to have enough surface contact to create a viable connection to be able to effectively measure contact between the body and a garment in this system.

Overall, the largest four sensors (2.54 cm, 1.905 cm, 1.27 cm, 0.635 cm) appear to be effective in and viable for detecting body-garment contact, as each sensor has a high voltage reading of at least 4V. However, the very smallest sensor (0.3175 cm), which is

very small, did not prove to be effective in detecting body-garment contact, as it has a very low voltage reading around 1V. This being true, a 0.3175 cm diameter conductive patch is simply too small to be used. Of the sizes tested, the smallest diameter conductive patch that could be effectively used in this method is 0.635 cm.

CHAPTER 6: APPLICATION TO LCG

6.1 Introduction

This method has been developed for the purpose of evaluating the fit and body-garment contact of current LCG/LCVG garments. Being able to measure body-garment contact in the current LCG/LCVG will provide data on problem areas that can be used in redesigning the base garment and tube layout.

One approach to implementing electrical contact sensors into an existing LCG/LCVG, is to integrate individual conductive patches directly onto the inside of the LCG/LCVG for testing purposes. These conductive patches would be temporarily attached on the inside of the garment and could be placed anywhere. This approach is advantageous because the conductive patches can essentially go anywhere (at any given time/trial) and they can be as close or as far away from each other as they need to be. This approach allows for a great amount of customization and being able to place contact spots over any area. However, it is a more labor-intensive approach as individual contact points must be implemented for each garment to be tested and the geometry and spacing of contact points may not be as consistent from test to test, limiting the ability to compare contact "maps" between garments.

Another approach would be to use a modular type method to test multiple different points in one particular area at a time, where a set of contact points (for example, in a grid pattern) is integrated into a textile swatch, which is then attached to the garment. These contact points would be consistent with each trial, as they are fixed in the same spot and only the textile that the sensors are attached to would be moving. This approach is less time consuming to implement, and allows the test system to be moved easily from

location to location.

Using either approach, selecting predetermined key areas of the LCG/LCVG in which to integrate conductive patches to evaluate body contact (e.g., for known problem areas or areas of recent redesign) would be a valuable step before actual implementation into the LCG.

Depending on the results desired, one approach might be more useful over the other. Clothing/body locations that have a large amount of sparse areas, spread out on the body that are of interest to evaluate might benefit from using the approach that allows placement of individual sensors in any location on the garment. That way the data could be collected in a smaller number of trials. On the other hand, clothing/body locations that have denser, smaller areas that are of interest to evaluate might benefit more from using the modular method. This method may require more trials, as the sensors are placed in a fixed configuration closer together, therefore only a small surface area can be tested at one time.

In both options, the wires that connect the conductive patch to the Arduino system would be lightly woven through the layers of the garment, in an attempt to eliminate potential interference and forces on the garment itself.

For this study, a modular grid of sensors was developed. This method has been implemented in a pilot test of a known problematic area that is relatively small in size and surface area on the torso. However, the benefit of a modular grid is that it can be placed anywhere, for as many trials needed, on the inside of a garment, in order to more fully evaluate the body-garment relationship.

6.2 Method

The Arduino Uno board used in this method has a total of six analog pins, therefore, that is the maximum number of sensors this system can be designed for. A grid of six patches has been created, sewing patches onto a textile by hand, and integrated onto a modular swatch which could be placed and moved anywhere inside the garment (Figure 6.1).

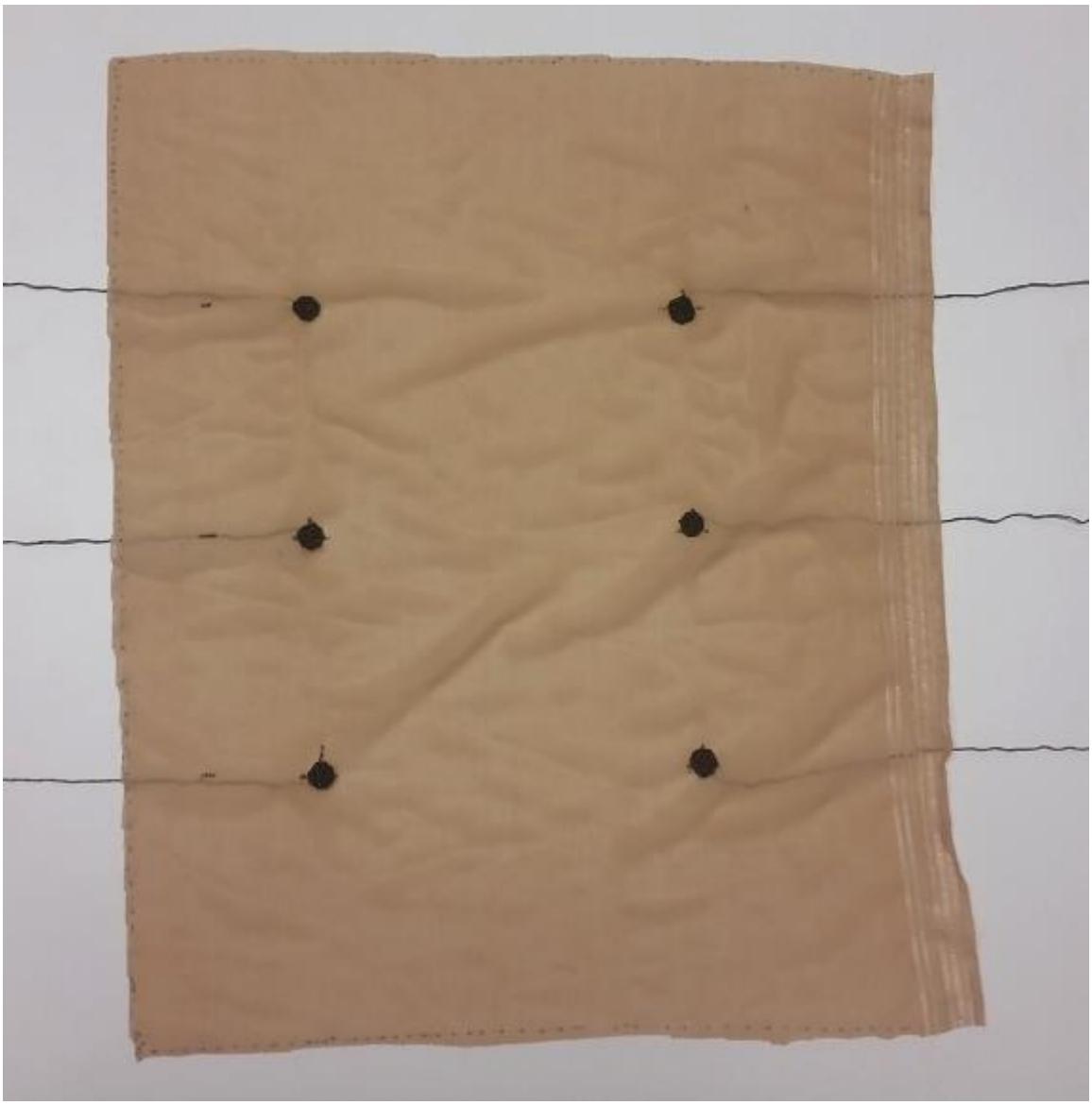

Figure 6.1: Sensor grid.

The swatch that contains the grid of six sensors was basted onto the inside of the LCG in the right-torso area, to temporarily secure it in place, and used to measure body-garment contact in the LCG during a series of EVA-like movements.

6.3 Grid Sensors

A grid of 6 sensors was created for the implementation into the LCG for contact testing. Patches were evenly positioned and mounted on a 25.4 cm long (wale direction) by 20.32 cm wide (course direction) single filling knit nude mesh textile using conductive thread to create a lead that connects to the microcontroller. Each sensor was attached to the mesh textile sewing by hand with 100% polyester non-conductive thread. The dimensions and placement of the sensors is pictured in Figure 6.2.

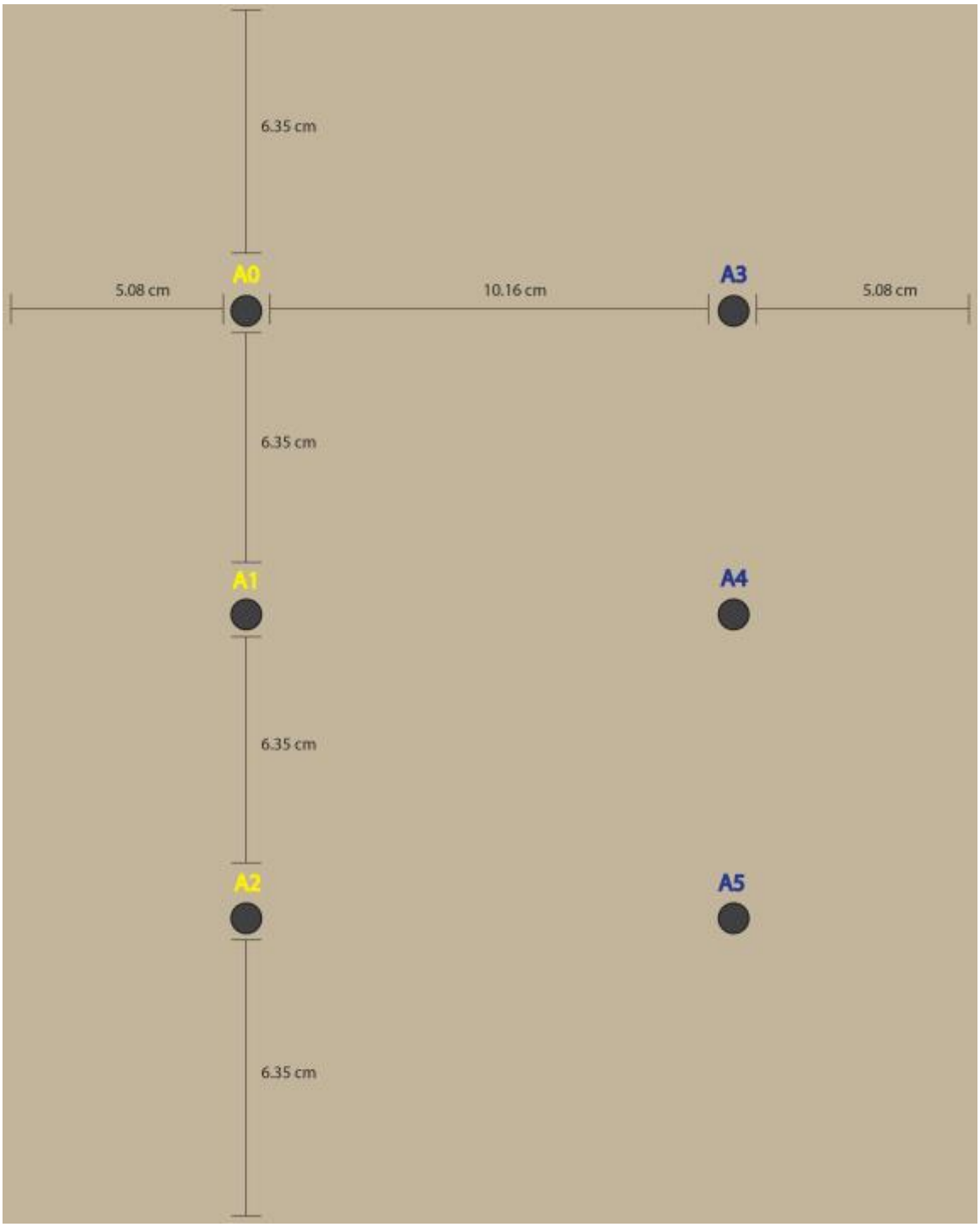

Figure 6.2: Grid sensors placement illustration.

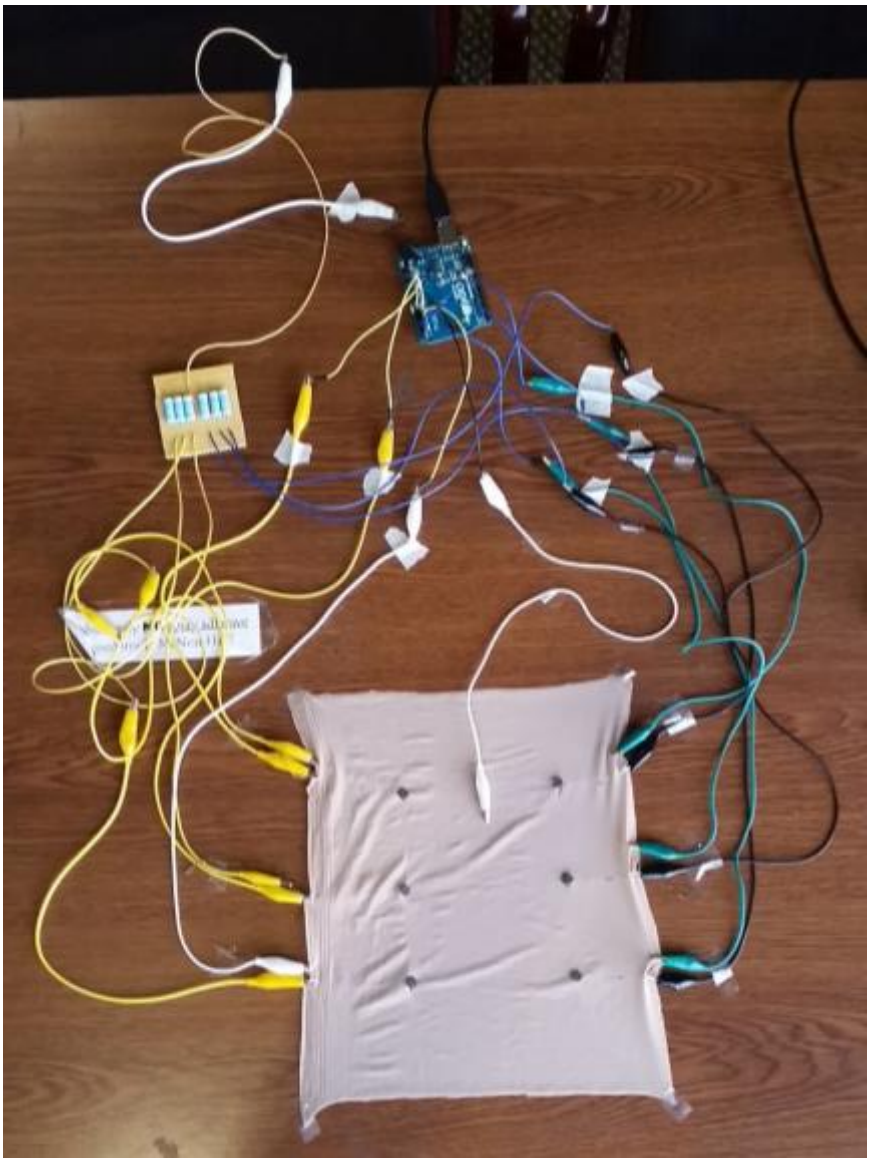

Figure 6.3: Grid sensors test set-up.

6.4 Testing: Grid Sensors

An initial test of the grid was performed to capture baseline performance and sensor interaction effects. A method similar to that used for the previous tests (conductive materials, contact force, and patch sizes) was used to test the grid sensors (Figure 6.3).

The sensor swatch was securely taped onto the surface of a flat tabletop. This time,

instead of simply holding the wire from the VCC pin, an electrode was adhered to either the right or left hand (depending on the sensors being tested) and an alligator clip coming from the VCC pin was connected to the electrode to create body connection. This is the same method that is used to create a connection with the body in the LCG implementation, but the electrode is placed in a different location on the body surface.

When testing sensors A0-A2, which are all located on the left side of the textile grid, the left hand/arm was used to create contact with the sensors. The electrode connecting the body to the Arduino was adhered to the top of the left hand.

When testing sensors A3-A5, which are all located on the right side of the textile grid, the right hand/arm was used to create contact with the sensors. The electrode connecting the body to the Arduino was adhered to the top of the right hand.

When testing all six sensors at one time, both arms were used to create contact (left arm for sensors A0-A2 and right arm for sensors A3-A5). The electrode was placed on the left hand.

Both single and multiple sensor contact tests were performed. Each sensor (A0-A5) was tested individually for contact. When each sensor was tested individually, the index finger of the respective hand that had the electrode adhered to was used to create contact between the body and the conductive patch (see Figure 6.4).

Figure 6.4: Testing one sensor.

Multiple sensors at once (A0-A2, A3-A5, and A0-A5) were also tested for contact. When multiple sensors were tested at the same time for contact, the underside of the lower arm was used to create the connection between the body and the conductive patch (see Figure 6.5).

Figure 6.5: Testing multiple sensors.

6.5 Data Analysis: Grid Sensors

Each trial from the grid sensor testing was recorded using the same method as the other tabletop tests performed earlier with conductive materials, patch force, and patch size. The results text file was imported into Microsoft Excel and graphed for visual analysis. A line graph was created for each trial. Averages and standard deviation of each

sensor (A0-A5) was calculated and also graphed using a bar chart.

6.6 LCG Implementation

After tabletop testing and analyzing of the data for the grid sensors was complete, the grid of six sensors was integrated onto the inside of an LCG that was provided by the Advanced Spacesuit Team at Johnson Space Center (JSC) (Figure 6.6). The tubing in the current LCG/LCVG runs primarily in the lengthwise (vertical) direction on the body, with the exception of the shoulder and upper leg regions where the tubes are positioned at a 45-degree angle to the lengthwise axis of the body. The torso is the center/core of the body, and thus produces a significant proportion of body heat. In addition, it appears to be a problematic fit area for the LCVG/LCG (Figure 2.6). Therefore, the torso is a high-potential location for an initial evaluation of the LCG/LCVG with this method. The grid was attached to the LCG on the right-side of the torso, by basting (a loose hand-stitch meant for temporarily securing things in place). Basting was used as the method for integration in order to securely (but temporarily) attach the swatch to the garment, to eliminate potential interference with the garment and its properties and to avoid damaging or permanently altering the base garment.

Figure 6.6: Grid sensors implemented on inside of LCG.

The body was connected to the microcontroller with an electrode that was adhered just underneath the center of the collar bone (Figure 6.7).

Figure 6.7: Electrode connecting body to microcontroller.

Various movements, similar to those that astronauts would perform during EVA, were tested. These movements are described in Table 2. For this pilot test, one female wear tester wore the LCG for all tests.

Table 2: List and description of movements testing in LCG.

Movement Number	**Movement Description**
Movement #1	Arm Circles
Movement #2	Kneeling on one knee (alternating sides)
Movement #3	Kneeling and touching the ground (alternating sides)
Movement #4	Picking up an object on the ground, turning, and placing object on a tabletop surface
Movement #5	Standing
Movement #6	Standing up from prone position
Movement #7	Toe touch with both hands
Movement #8	Touching toe with opposite hand (alternating sides)

These movements include a variety of body positions, and are likely to illustrate different amounts of contact between each sensor location on the garment and the body.

6.7 Data Analysis: LCG Implementation

From the tabletop testing results of the grid sensors, using the highest voltage value of a sensor that was not in contact (false positive) and the lowest voltage value of a sensor that was in contact, a threshold binary voltage value has been calculated to determine body contact or noncontact. The value that is in-between the highest false

positive value and the lowest value of a sensor that was in contact with the body is the threshold. The highest binary voltage value of a sensor that was not in contact with the body was 344 (1.68V) and the lowest binary voltage value of a sensor that was in contact with the body was 544 (2.66V). The binary voltage value that is in-between these two values is 444 (2.17V), which has been used as the threshold to determine contact vs. noncontact in this method for analysis.

A total of eight trials were recorded, one for each movement performed (total of eight movements). Each movement was recorded as a separate trial. At the beginning of each trial a force was manually applied to each sensor by the wear tester from the outside of the garment using the index finger for calibration and verification purposes. This ensures that each sensor is responding to body-garment contact. This calibration process started with the first sensor (A0), continued through each subsequent sensor, and ended with the last sensor (A5). Force was applied to each sensor for about five seconds, with a resting period of approximately five seconds following each period of applied force. After the calibration process for each trial was completed, the specified movement for each trial was performed.

The data from the LCG tests were collected in the same way as the previous tests (conductive materials, contact force, and patch size), using the Arduino Uno and CoolTerm™. Results text files were imported into Microsoft Excel and graphed using a line graph. Using the threshold described previously in this section, periods of contact and non-contact for each sensor were calculated and expressed as an overall contact percentage for each sensor in each trial. Averages of each sensor contact percentage for

each trial were calculated and graphed using a bar chart.

6.8 Results: LCG Implementation

The test results for each individual sensor (A0-A5), as well as test results for a combination of multiple sensors at one time are illustrated below in Figures 6.8-6.16.

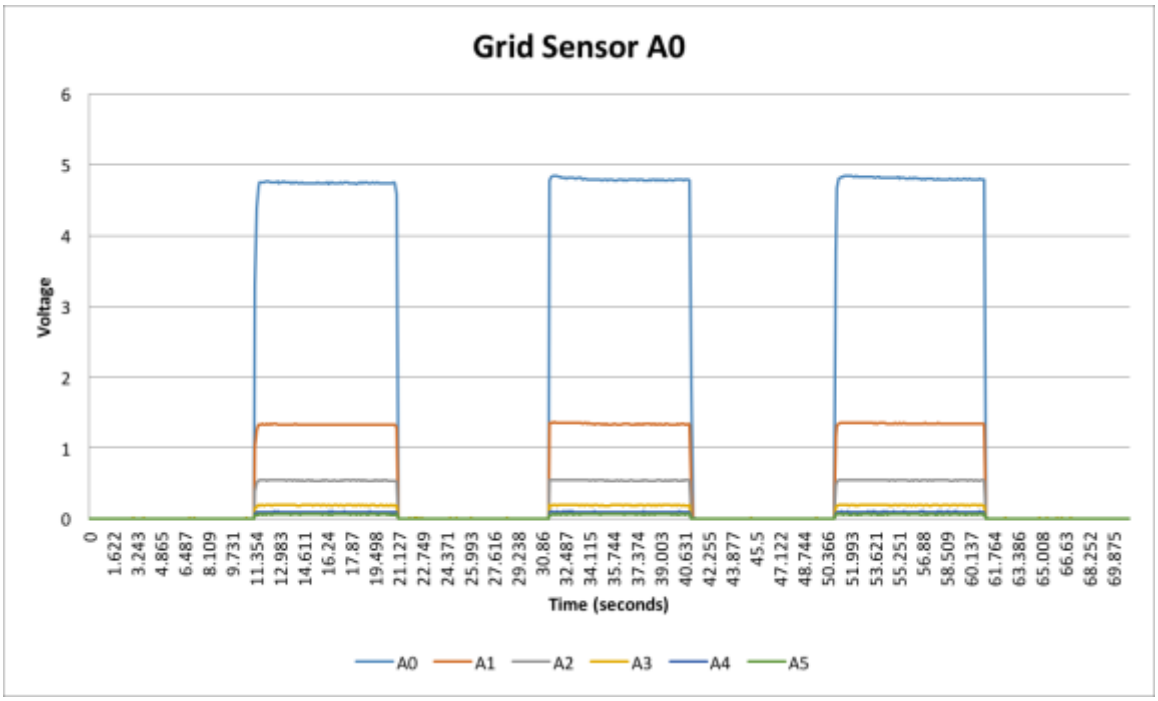

Figure 6.8: Contact test sensor A0.

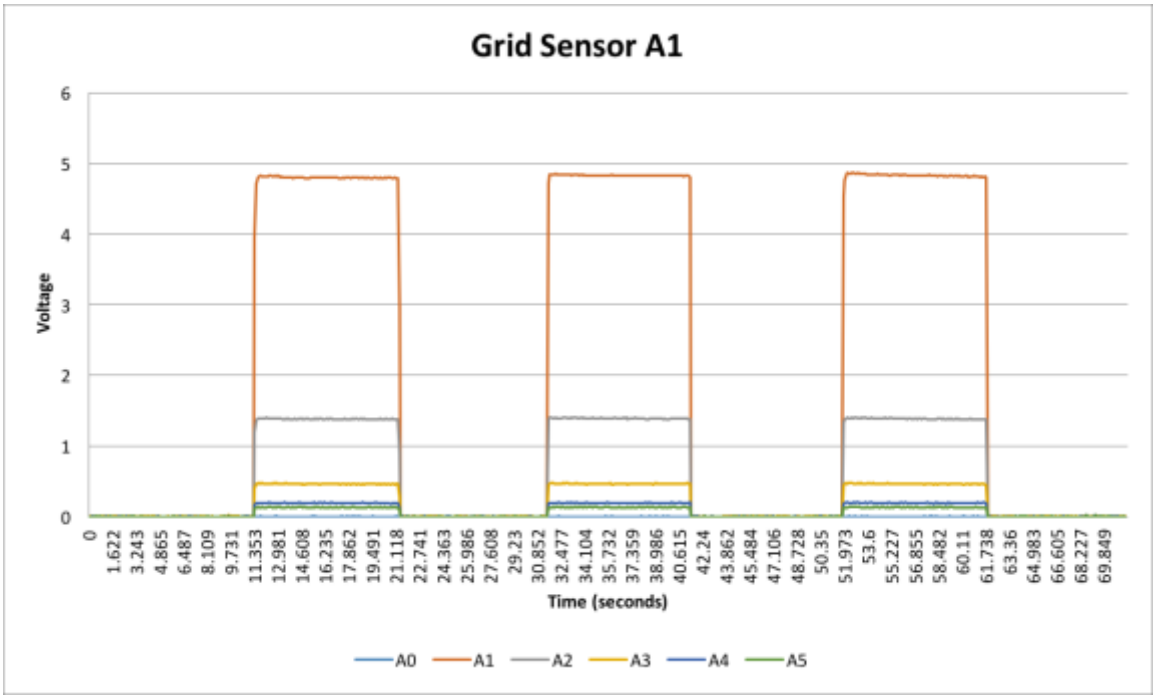

Figure 6.9: Contact test sensor A1.

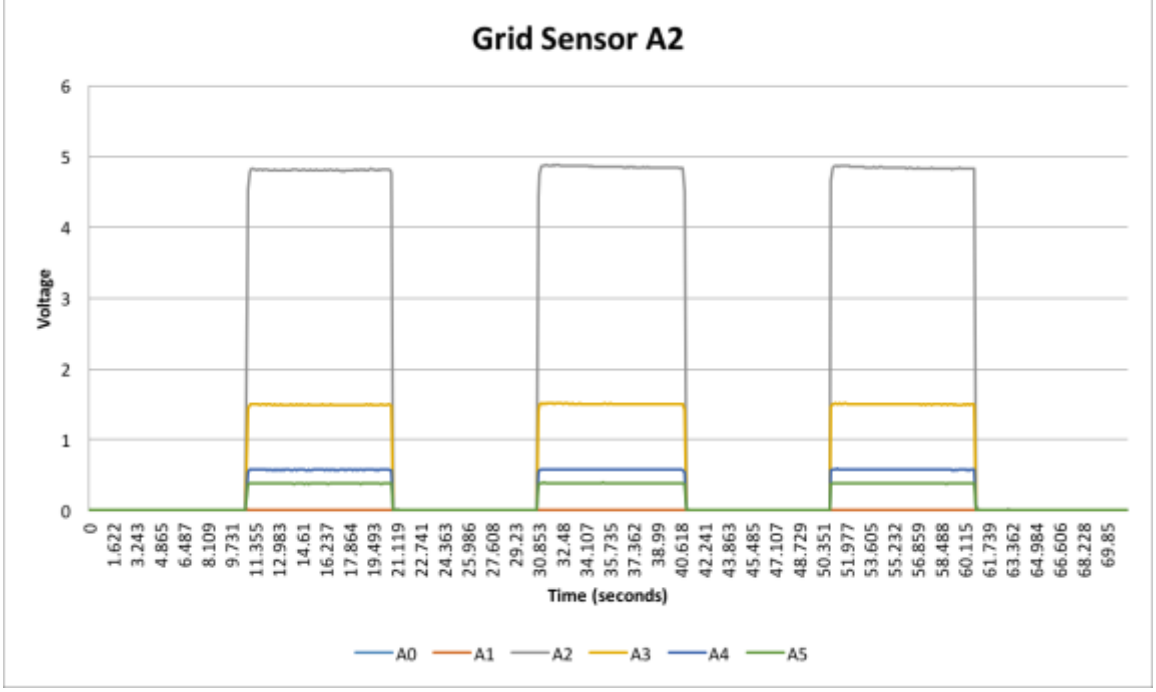

Figure 6.10: Contact test sensor A2.

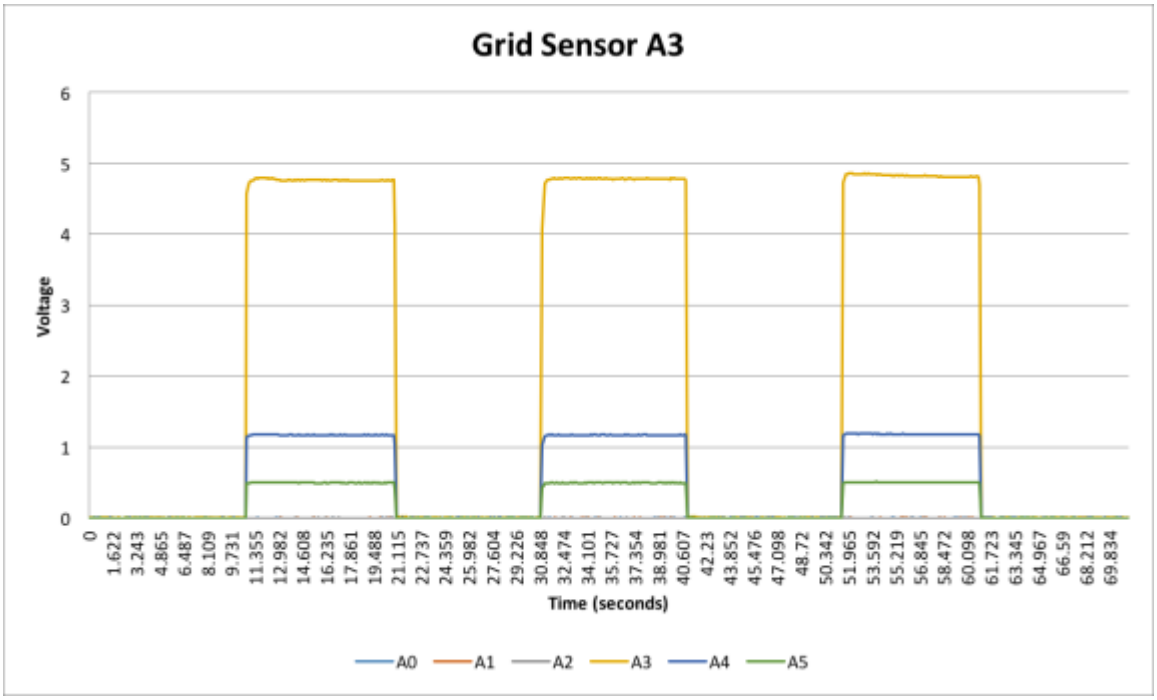

Figure 6.11: Contact test sensor A3.

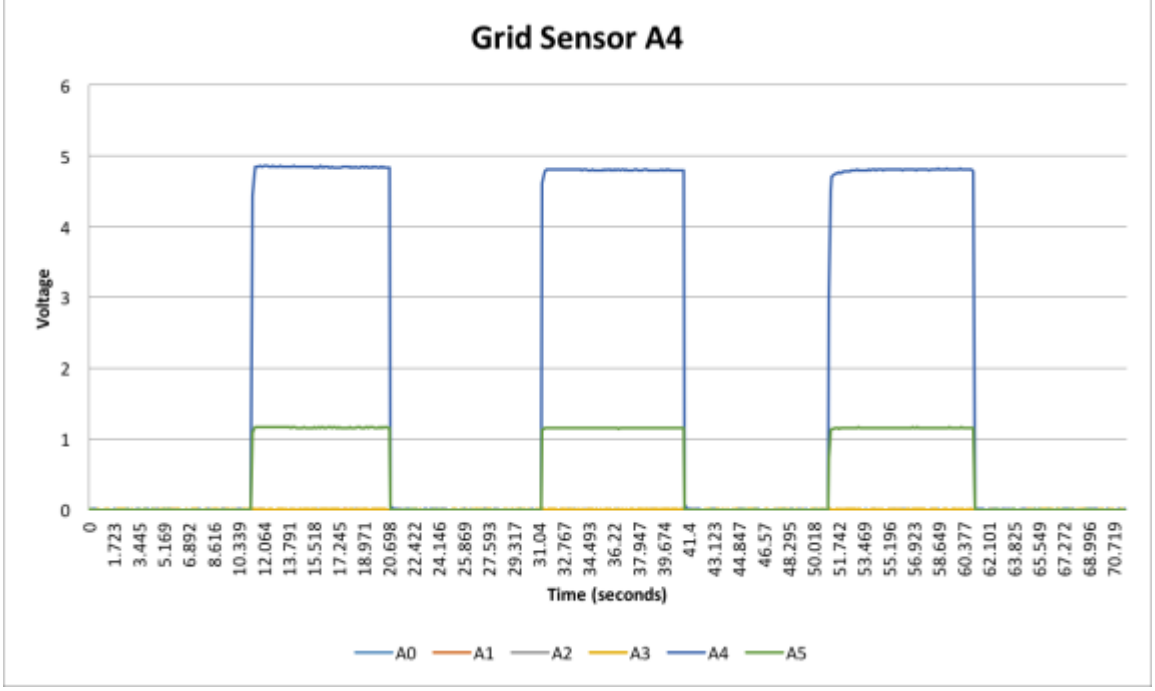

Figure 6.12: Contact test sensor A4.

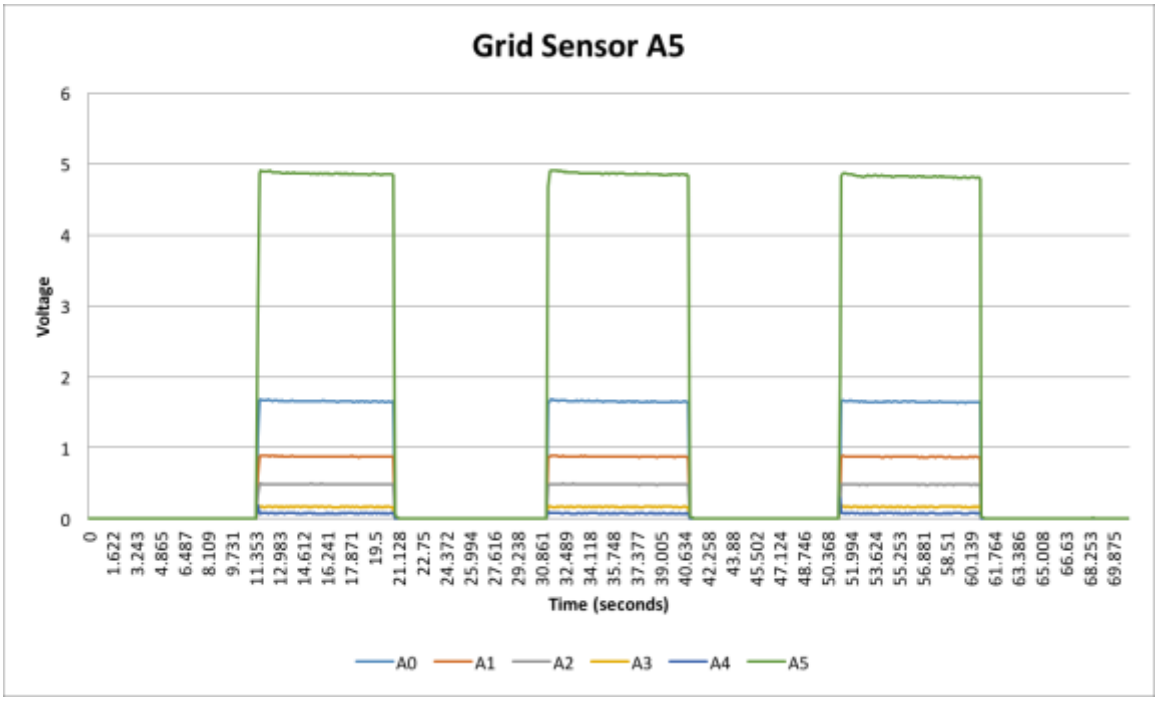

Figure 6.13: Contact test sensor A5.

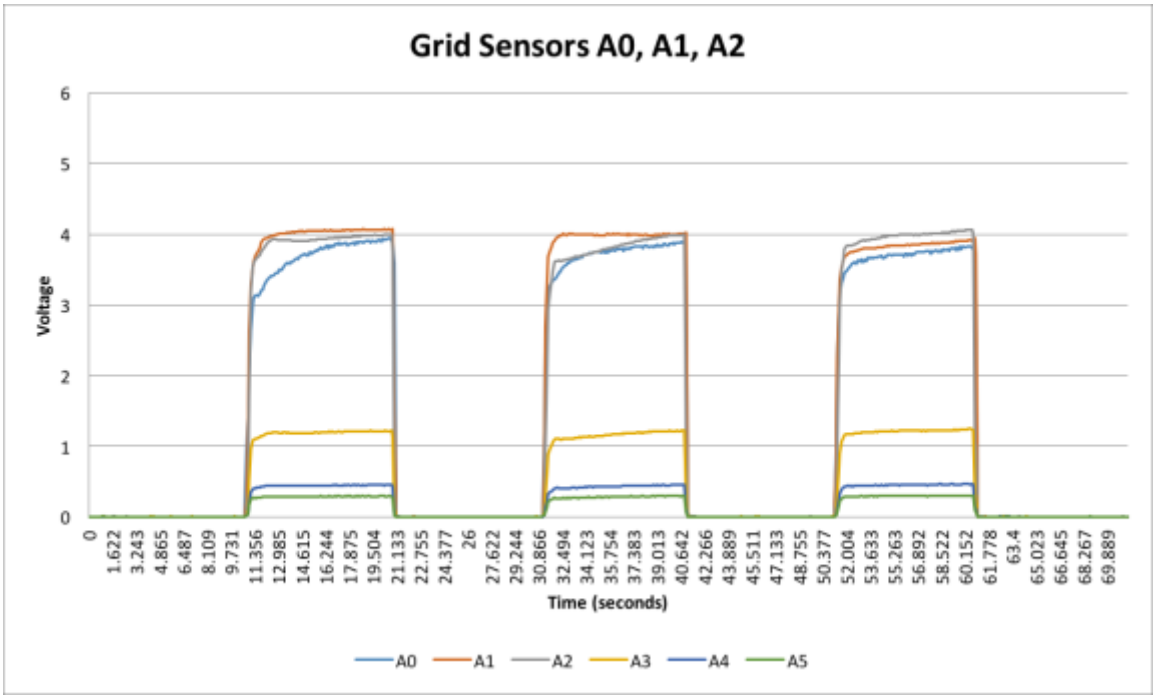

Figure 6.14: Contact test sensor A0, A1, A2.

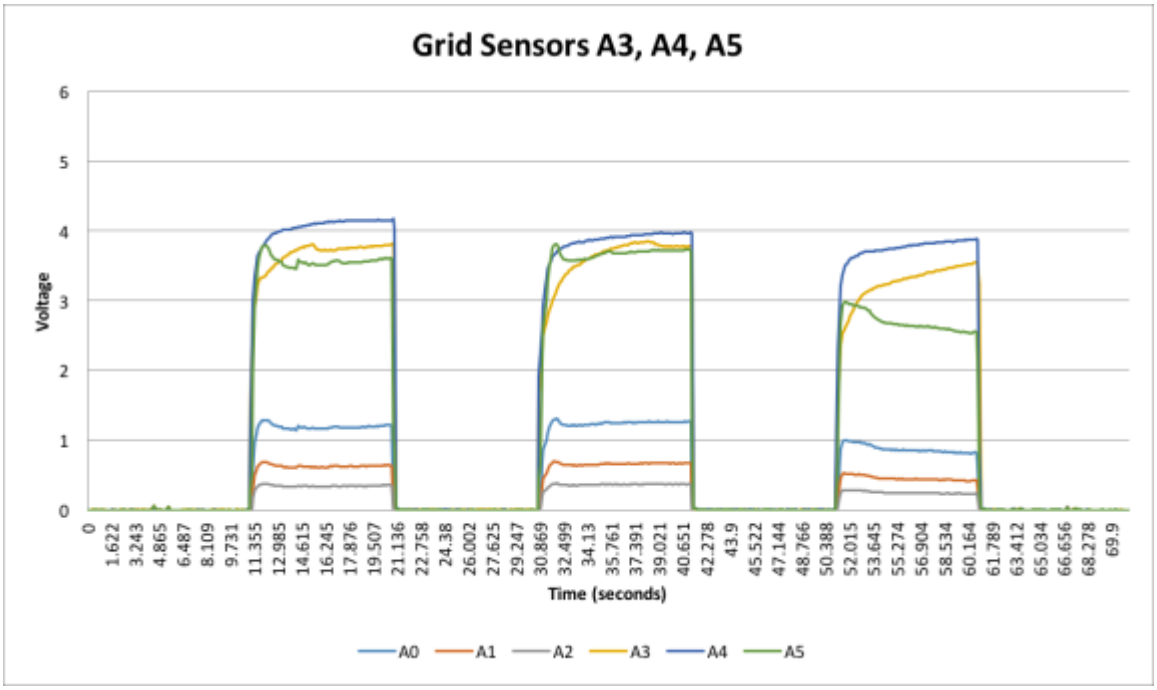

Figure 6.15: Contact test sensor A3, A4, A5.

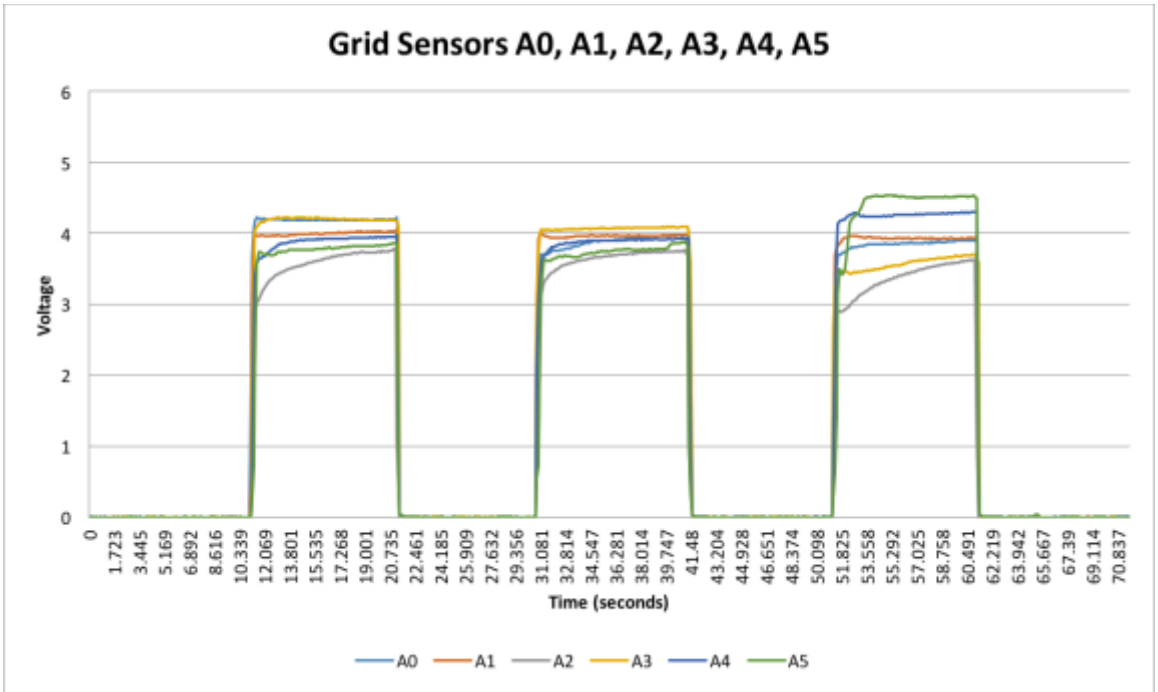

Figure 6.16: Contact test sensor A0, A1, A2, A3, A4, A5.

The bar graph (Figure 6.17) depicts the average percentage of body-garment contact for each movement/trial and sensor.

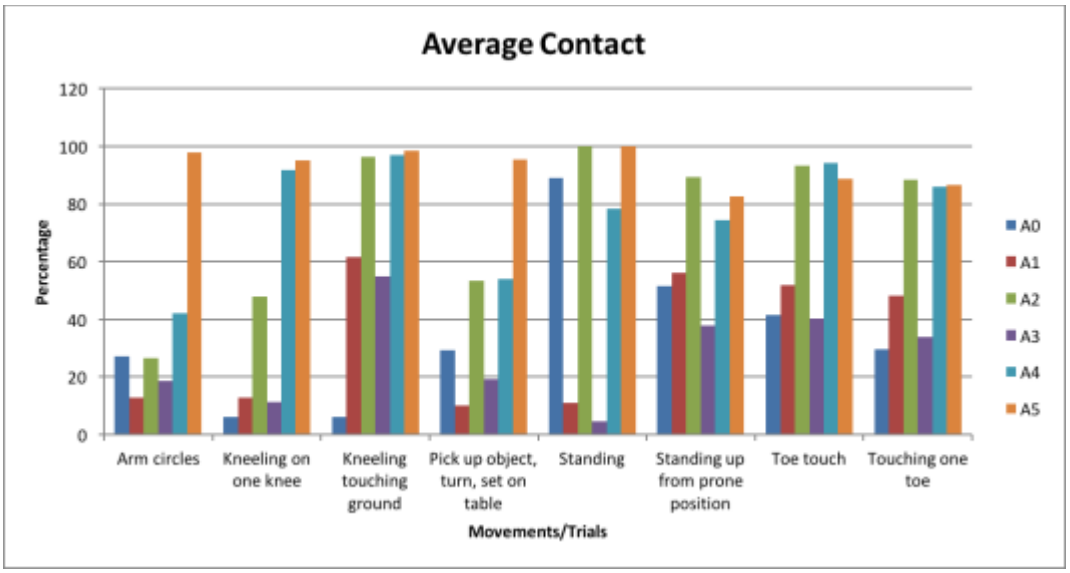

Figure 6.17: Average sensor contact in LCG.

6.9 Discussion

6.9.1 Sensor Grid

The results of the sensor grid testing showed that each sensor responded to measuring body-garment contact. Contact with some sensors appeared to create a slight increase in voltage for other sensors that were not in contact with the body. This could potentially be due to the wear tester's arm being close to the other sensors. However, there is a noticeable difference shown for sensors that are in contact versus sensors that are not in contact with the body. This information was used in the calculation of the threshold contact voltage used to measure periods of contact and non-contact in the

garment-integrated test.

6.9.2 LCG Implementation

The results of LCG testing with the grid sensors showed that some sensors overall exhibit very good contact as well as some sensors having good contact only for certain movements and having poor contact for other movements. Figure 6.18 shows sensor locations on the female wear tester's body.

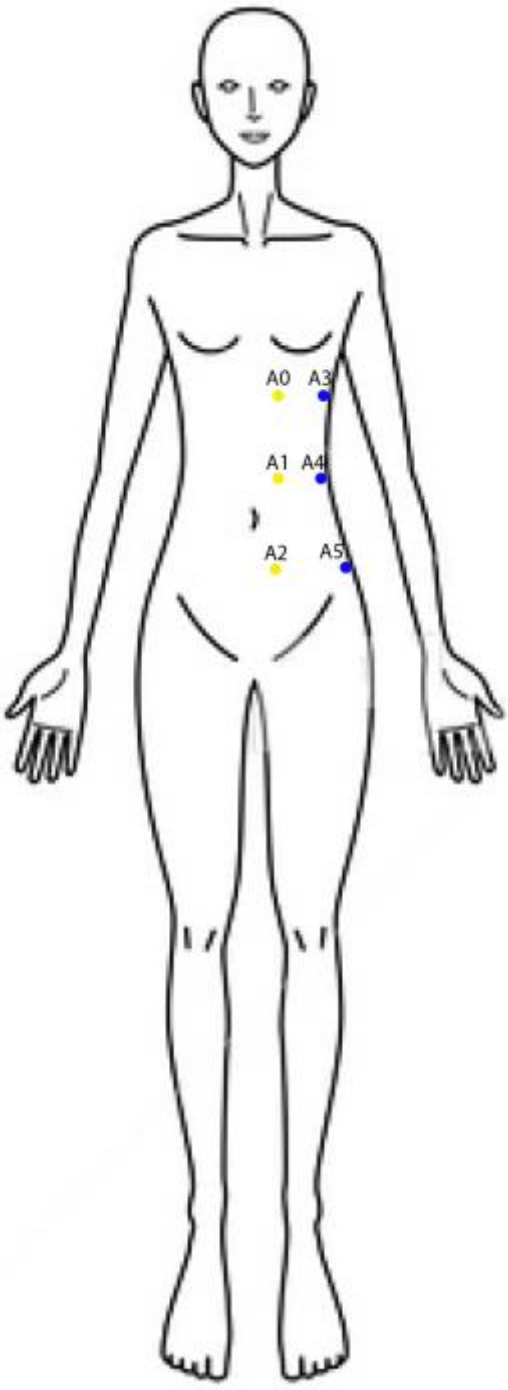

Figure 6.18: Sensor locations mapped on female body.

(Mannequin illustration from https://www.pixtastock.com, 2016)

Sensor A5 was consistently the highest contact sensor for all trials. This sensor was located at the side of the body near the iliac crest (hip bone). Its location may be the reason why it had the strongest connection with the body. On the body the hips are typically one of the widest areas for female and (depending on different body shapes) can create a significant protruding curve from the waist, and in some cases a prominent localized protrusion due to the iliac crest. This is especially true and most extreme at the lateral hip. This protruding area may have afforded better and more consistent contact with the garment, resulting in a higher percentage of contact time. Sensor A5 may have been in contact with the body for a larger percentage of the time because the hip is placing a natural force on the garment, simply due to the body's geometry. This force creates a contact with the body that does not easily move out of place. Another factor is that the pelvis is a boney structure. This may facilitate solid body-garment contact, depending on amount of overlying muscle and fat.

Other sensors that displayed good contact overall were sensors A2 and A4, the two sensors closest to A5. Sensor A2 is in a similar location as sensor A5, but it is closer to the anterior midline of the body versus the side of the body. Sensor A4 is directly above sensor A5, on the side of the body. It is understandable that sensor A2 also exhibits a strong response, as it is in the region of in the bony hip. However, the good response from sensor A4 is interesting, because it is located near the side of the body in the middle (natural waist) of the stomach vertically. This is the part of the body where the natural waist typically falls (though varies greatly with as body shape and size), and one might assume there would be poor contact there because of the natural concave shape that the

waist creates. Sensor A4 had the weakest average during both the arm circles and picking up an object, turning, and setting object on table. Both of these movements involve a great deal of arm and shoulder movement, which could be contributing to the poor connection. It could be that while extending the arm (either up for arm circles or out in front of the body to pick something up or set something down) the garment pulls away from the body to allow body extension to take place.

Sensors A0, A1, and A3 all showed the weakest response and lowest average contact with the system. Sensor A0 is the top sensor on the right side of the sensor gird, near the center front of the body. This sensor showed a poor response for all of the movements except for standing. With wear tester standing, sensor A0 had a very good connection with the body. This might mean that contact between the body and a garment is maintained during static positions, but not mobile positions. Sensor A1 is located directly below sensor A0 and Sensor A3 is located near the top side of the body. It could potentially be that the concave shape and placement of the waist in combination with the convex shape and placement of the breast creates a gap around this area, particularly right underneath the breast. This does not appear to be an issue with the convex shape of the hip, as it does not protrude out as much and is generally a more "flat" convex shape, rather than a "round" convex shape. Another reason this area is problematic is that the garment may not be designed for a women's body. Most functional garments are sized as a unisex system, and unisex sizing is developed from men's sizing. This can lead to issues with fit, mobility and, comfort. An LCG/LCVG designed specifically for women would most likely fit better and therefore have stronger connections throughout the

garment.

6.9.3 Overview

Overall the three sensors (A2, A4, and A5) that are located in the bottom left side of the sensor grid, show the strongest average connection with the body. In contrast, the three sensors (A0, A1, and A3) that are located in the upper right side of the sensor grid showed the weakest response and average contact with the body. The results from this method appear to be useful in measuring the dynamic fit of the LCG.

6.9.4 Limitations

A significant limitation of this study is that only one wear tester was used as the fit model. Therefore, only one body shape and size was tested. This will affect the fit of the garment and the body-garment contact. Having multiple models would be useful to assess the validity of this method.

Another limitation is the question of variable contact force and how it affects the data. Although the effect of contact force was evaluated, the test performed was so coarse that it could only determine that more force than just patch weight was needed to register a body-garment contact. However, this result shows that light contacts will not be registered by this system, even though they may be in fact body-garment contacts.

Due to the size of sensor grid tested, very small or complex shaped areas may not be suitable for this particular grid of sensors. If a smaller or more complex shaped area is desired to be tested (armscye, neckline, crotch area), a smaller sized grid should be used to evaluate body-garment relationship. The layout of the sensor grid can be changed,

allowing it to be any size desired.

Finally, another significant limitation of this study is the absence of a gold-standard measure for comparing. It is unknown whether this method is capturing body-garment contact accurately. A comparison measure or a better characterization of the effects of contact force would help inform if this method is measuring body-garment contact accurately.

6.10 Implications for LCG/LCVG Redesign

A key use for this method of measuring contact would be in comparative evaluation of new LCG/LCVG tube layout designs. Arthur Iberall developed an approach in 1947 at the National Bureau of Standards (offered to David Clark Company in 1951) that could be successfully implemented to create tube placements that are less likely to be subject to forces during body movement that pull the garment surface away from the body. His research identified lines of non-extension (see Figure 6.19), which are lines on the body surface where body movement essentially will not cause stretching or contraction. Iberall's focus was facilitating mobility in full-pressure suits and mechanical counter-pressure garments. Iberall's lines of non-extension are currently not aligned with the tubing layout of the LCG/LCVG, and work against the principle (see Figure 6.20). This approach has proven to be useful in previous space technology research, innovation, and development, and thus can provide solutions for the effectiveness of the LCG/LCVG today (Iberall, 1964).

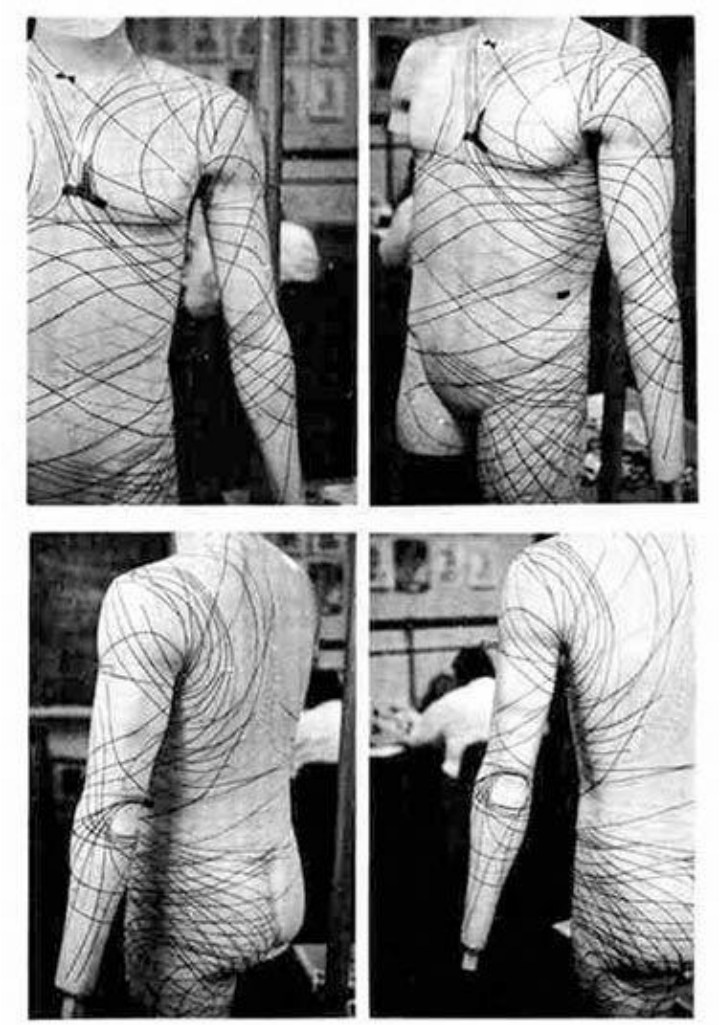

Figure 4

Lines of nonextension for the upper part of the body

Figure 6.19: Iberall's LoNE.

(Iberall, 1964)

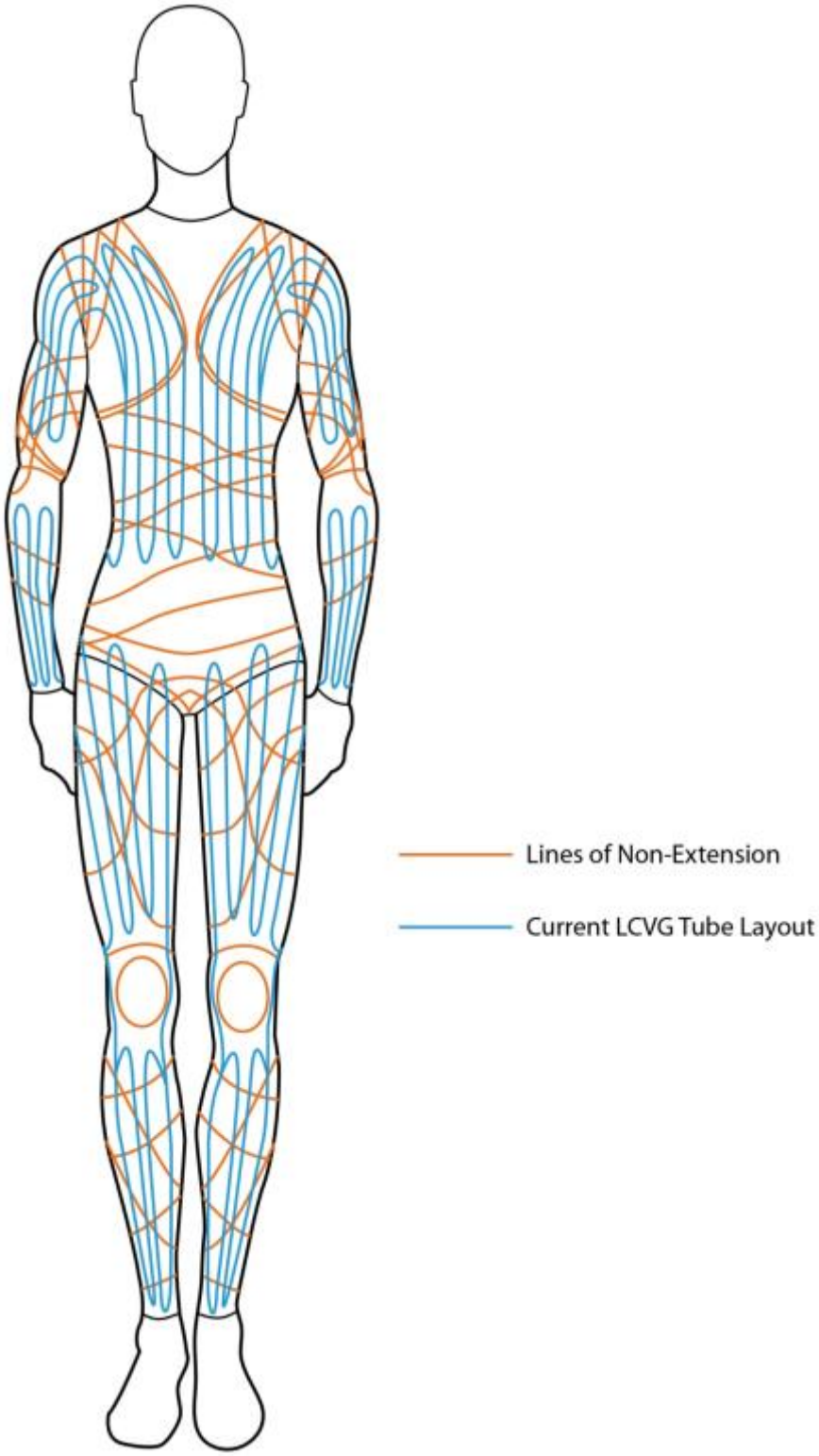

Figure 6.20: LoNE and LCG/LCVG tubing layout mapped on body.

A tube layout based on Iberall's LoNE and a functional apparel patternmaking approach, are likely to improve the body contact of the LCG/LCVG tubing. The tubes used in the LCG/LCVG are fairly non-pliable and do not stretch. Therefore, ideal placement of tubes within a garment that is worn on the body, are in locations on the body that do not stretch, contract, or deform. Iberall's LoNE theory provides insights as to where these areas are on the body (Iberall, 1964). Ideally, applying this theory could improve the mobility and body-garment contact of the LCG/LCVG, and by extension, the efficiency and effectiveness of it.

The breathability of the LCG/LCVG materials is another factor that could affect the thermoregulation of the garment. Additionally, the stretch and structure of each individual material will have an effect on the mobility and comfort of the wearer, and as a result, the effectiveness of the LCG/LCVG.

Using the smallest diameter of tubing possible could offer improvements to the LCG/LCVG in many areas, such as, mobility, performance, comfort, and effectiveness.

The performance of a redesigned prototype LCG/LCVG can be compared to that of an existing LCG/LCVG, by using the evaluation method presented here.

6.11 Implications for Other Applications

Form fit is not strictly a unique problem to the LCG/LCVG itself. Other applications where form fit is an important aspect of the garment are garments for scuba divers, sprinters, downhill skiers, and ski jumpers. Athletes who participate in these sports rely on the tight form fit that contribute to performance of the garment(s) they wear.

Other user groups that use cooling technology apparel are racecar drivers and pilots. Hot environments are typical for these individuals who need to have their core body temperature regulated.

This LCG/LCVG application has benefits not only for NASA and future space exploration, but also for other applications that also rely on similar technology and development.

CHAPTER 7: CONCLUSION

7.1 Conductive Materials

Material #7 (Conductive Hook Fastener) proved to be the most promising material to measure body contact to garment. However, Material #7 is a conductive "hook" fastener and is relatively rough and scratchy. It is the coarsest material that was used in this study. The stiffness and protruding hooks of this material may facilitate better contact with the body than materials that are soft, smooth, and light. Though this material has a high correlation with the reference signal, it may not be the most feasible for long-term wearable solutions, as with long-term exposure to the skin, it may cause skin redness and irritation. However, this method requires only short wear periods.

The second most promising material for measuring body-garment contact is the other fastener material, Material #8 (Conductive Loop Fastener), which is the conductive "loop"-side fastener. This material is similar to Material #7 (Conductive Hook Fastener), as they both have protruding surface textures. However, Material #8 (Conductive Loop Fastener), which is composed of loops instead of hooks, is much softer and is less scratchy than Material #7 (Conductive Hook Fastener).

The surface texture of a material appears to have an effect on the quality of electrical contact. For example, with the fastener material samples (Material #7 (Conductive Hook Fastener) & #8 (Conductive Loop Fastener)), there are small protruding areas (rather than a broad flat area) that seem to localize the contact force in those areas. It's possible that this causes an increase in pressure, which makes a stronger electrical connection (a lower resistance to electrical current), resulting in a higher correlation between the voltage signal and the reference signal.

Another material property that seems to have an effect on measuring body-garment relationship is density/thickness and/or rigidity of the material. The more dense or rigid a material is, as in Material #1 (Stretch Conductive Fabric), #2 (Copper FlecTron Conductive Fabric), and #3 (Nickel Mesh Conductive Fabric), the more consistent the body-garment electrical signal is, and thus, the higher the correlation between voltage signal and reference signal. Similarly, stiffer textiles appeared to provide more consistent signals. Despite Material #3 (Nickel Mesh Conductive Fabric) being an open-weave textile, its rigidity is similar to that of Material #2 (Copper FlecTron Conductive Fabric). These two textiles provided similar responses to body-garment contact.

Material #6 (EX-STATIC Conductive Fabric) showed the weakest performance for measuring body-garment contact, as evident in its weak correlation with the reference signal (an implication that it does not facilitate a good electrical contact with the body). This is most likely due to the fact that this material has a relatively low proportion of conductive material in its composition. The conductive fibers in this textile are woven sparsely in a small diamond shape pattern.

Material #1 (Stretch Conductive Fabric), #2 (Copper FlecTron Conductive Fabric), #3 (Nickel Mesh Conductive Fabric), #4 (High Performance Silver Mesh Conductive Fabric), and #5 (Fine Mesh VeilShield Conductive Fabric), are feasible options to measure body-garment contact, as they show a clear response to body contact and relatively strong correlations with the reference signal (r-squared values around 0.7) (Figure 4.9). The emphasis of this investigation was to determine if a binary-type measurement of body contact was feasible (detecting either contact or noncontact), all of

these materials appear to show variable voltage responses to constant body contact, which would imply that in a measurement scenario each material may require a different threshold voltage for determining "contact." In some cases, the variability in contact-voltage may make certain materials more error-prone. However, initial evaluation of the electrical response graphs shows the possibility that an analog electrical response to contact force may be present. Further study is needed to determine if the relationship between force and voltage can be reliably characterized and used to measure not only the presence of contact but also the force of contact.

Overall, from the results of this study, materials with low resistivity appear to be able to measure body-garment relationship more effectively and consistently, compared to materials with higher resistivity. The surface texture of the material also played a role in the effectiveness of the body-garment contact. Materials that had a rougher texture had a stronger signal compared to materials that had a smoother texture. Materials that appeared to be less effective at measuring body-garment contact were characterized as: higher resistivity, lower proportion of conductive materials, and lightweight or very flexible properties. Materials that have a higher density and rigidity, with a low resistivity, appear to be the most successful materials for measuring body-garment relationship. Materials that have a lower resistivity and flexible or lightweight properties are less suitable for effectively measuring body-garment relationship.

7.2 Contact Force

Two methods of applying force between the body and the sensor were evaluated. The first test evaluated the contact created by arm weight on top of the sensor, and the

second test evaluated the contact created by the weight of the sensor on top of the arm.

The results from these tests showed that contact force applied to the connection between the body and the sensor had a significant effect on the output of the system. Further investigation is needed to fully understand the effects of force in this system and the limits of the method.

7.3 Patch Size

Five conductive patch sizes were tested for their effectiveness in this system. The objective was to determine the smallest sized diameter for the conductive patch while still being able to detect body-garment contact. The five patch diameters were: 2.54 cm, 1.905 cm, 1.27 cm, 0.635 cm, and 0.3175 cm.

All sizes, with the exception of the smallest size conductive patch (0.3175 cm), appear to be viable in effectively capturing the body-garment relationship. The voltage response of each sensor is slightly different. However, the response (for the viable sensors) was at minimum 4V during contact, which is relatively high for this system with ability to measure contact and noncontact with the body.

This investigation sought the smallest viable patch diameter, in order to minimize the invasiveness of the patch. Using the smallest possible sensor in the LCG/LCVG provides the least amount of potential interference with the garment fit and cooling functions.

The 0.635 cm diameter circle conductive patch was used for testing in the LCG, due to its small size and effectiveness.

7.4 LCG Fit Evaluation

A grid of contact sensors was integrated (by basting) onto the inside of an existing LCG to measure body-garment contact with the method developed in this study. Results from the sensor grid testing showed that each sensor was able to capture and detect body-garment contact. The grid of six sensors was integrated onto the inside of the LCG in the wear tester's abdomen area on the right of the sagittal plane. Results of the LCG testing showed that sensors near the right hypochondriac region showed poor contact. However, in contrast, the sensors that were located near the right iliac region had much stronger contact as recorded by the system.

7.5 Limitations

Though this method has shown to be promising for measuring the dynamic body-garment relationship, specifically with a binary measure of contact/noncontact, a key limitation of this study is the lack of precise control of the amount and consistency of pressure applied between the wear tester's arm and the conductive patch. Inconsistent pressure between a body and a garment during movement is expected, and therefore, characterization of the relationship between applied force and voltage response for this system is needed. Further, it is not currently known what minimum amount of force between garment and body would be required for effective detection of contact, and therefore the results obtained from LCG testing cannot be reliably interpreted – it is possible that body-garment contacts below the threshold voltage level were not recorded. Force between the body and a garment may vary across locations and over time. Further research on this relationship would be useful to ensure that inconsistent pressure between

the body and the conductive patch is not a confounding variable.

Evaluation of this method was tested with only one wear tester. This is a significant limitation, because body size and shape vary, thereby affecting the body-garment relationship. Body shape and size varies by individuals and gender. The system should be tested on body sizes, shapes, and on both genders.

Material comfort could be improved for this method. A conductive hook fastener was used as the sensor material in this system, due to its very strong signal response. However, this material is quite rough and scratchy and has the potential to cause skin irritation, especially if testing is occurring over a long period of time. Material #8 (Conductive Loop Fastener), the other fastener material, would be a better alternative to the rough and scratchy Material #7 (Conductive Hook Fastener), as the loop fastener is much smoother and soft. This material also had the second strongest response, therefore may be as effective in measuring body-garment contact.

The tubes and the excess of fabric on the inside of the LCG are another limitation of this study, having the potential to interfere with the body-garment contact signal. Incorporating the sensor grid into the LCG can be difficult and not precise, as the LCG wrinkles when off bodies.

Variables related to the person wearing the LCG that might have an effect on the results of these tests are body temperature, body hair amount, hydration levels, and electrolyte levels. This test also did not control for the temperature sensitivity of the conductive test materials. Understanding how and to what degree these variables affect the results will be important in future characterization of this method.

Further investigation is indicated to ensure that this method is viable in accurately measuring body-garment contact. However, from this pilot investigation, the method appears to provide valuable information that can be used to better understand the relationship of the body and garment. This method is much less expensive and more accessible than other methods that are currently used and is relatively easy to implement into a garment.

REFERENCES

Arens, E., & Zhang, H. (2006). The skin's role in human thermoregulation and comfort. In N. Pan, & P. Gibson, *Thermal and Moisture Transport in Fibrous Materials* (pp. 560-603). Woodhead Publishing.

Ashdown, S., Loker, S., & Rucker, M. (2007, June). Improved Apparel Sizing: Fit and Anthropometric 3D Scan Data. *National Textile Center Research Brief*, 1-3.

Bayes, S. A., & Roebelen, Jr., G. J. (1992, March 3). *Patent No. 5,092,129.*

Cao, H., Branson, D. H., Peksoz, S., Nam, J., & Farr, C. A. (2006). Fabric Selection for a Liquid Cooling Garment. *Textile Research Journal*, *76*(7), 587–595. doi.org/10.1177/0040517506067375

Carson, M. A., Rouen, M. N., Lutz, C. C., & McBarron, II, J. W. (n.d.). *EXTRAVEHICULAR MOBILITY UNIT*. Retrieved 2016, from SP-368 Biomedical Results of Apollo: http://history.nasa.gov/SP-368/s6ch6.htm

Charkoudian, N. (2003). Skin Blood Flow in Adult Human Thermoregulation: How It Works, When It Does Not, and Why. *Mayo Clinic Proceedings*, *78*(5), 603–612. doi.org/10.4065/78.5.603

Chen, L., Hoey, J., Nugent, C. D., Cook, D. J., & Yu, Z. (2012). Sensor-Based Activity Recognition. *IEEE Transactions on Systems, Man, and Cybernetics, Part C (Applications and Reviews)*, *42*(6), 790–808. doi.org/10.1109/TSMCC.2012.2198883

Crocker, J. F. (1969, March 4). *Patent No. 3,430,688.*

Drewniak, E. I., Crisco, J. J., Spenciner, D. B., & Fleming, B. C. (2007). Accuracy of circular contact area measurements with thin-film pressure sensors. *Journal of*

Biomechanics, *40*(11), 2569–2572. doi.org/10.1016/j.jbiomech.2006.12.002

Fan, J., Yu, W., & Hunter, L. (2004). *Clothing Appearance and Fit: Science and Technology*. Woodhead Publishing.

Fiala, D., Lomas, K. J., & Stohrer, M. (1999). A computer model of human thermoregulation for a wide range of environmental conditions: the passive system. *Journal of Applied Physiology*, *87*(5), 1957–1972.

Fish, R. M., & Geddes, L. A. (2009). Conduction of Electrical Current to and Through the Human Body: A Review. *Eplasty*, *9*, 407–421.

Gavin, T. P. (2012). Clothing and Thermoregulation During Exercise. *Sports Medicine*, *33*(13), 941–947. doi.org/10.2165/00007256-200333130-00001

Gupta, D. (2011). Design and engineering of functional clothing. *Indian Journal of Fibre & Textile Research*, *36*(4), 327–335.

Gupta, D. (2011). Functional clothing— Definition and classification. *Indian Journal of Fibre & Textile Research*, *36*(4), 321–326.

Gupta, D., & Zakaria, N. (2014). *Anthropometry, Apparel Sizing and Design*. Elsevier.

Hensel, H. (1973). Neural processes in thermoregulation. *Physiological Reviews*, *53*(4), 948–1017.

Hong, L., Dongsheng, C., Qufu, W., & Ruru, P. (2011). A study of the relationship between clothing pressure and garment bust strain, and Young's modulus of fabric, based on a finite element model. *Textile Research Journal*, *81*(13), 1307–1319. doi.org/10.1177/0040517510399961

Iberall, A. S. (1964). *THE USE OF LINES OF NONEXTENSION TO IMPROVE*

MOBILITY IN FULL-PRESSURE SUITS.

James, D. (2016). *The Primary and Secondary Life-Support Systems*. Retrieved 2016, from NASA Quest: http://quest.nasa.gov/space/teachers/suited/5emu4.html

James, D. (2016). *The Space Shuttle Extravehicular Mobility Unit (EMU)*. Retrieved 2016, from NASA Quest: http://quest.arc.nasa.gov/space/teachers/suited/5emu1.html

Jordan, N. C., Saleh, J. H., & Newman, D. J. (2006). The extravehicular mobility unit: A review of environment, requirements, and design changes in the US spacesuit. *Acta Astronautica*, *59*(12), 1135–1145. doi.org/10.1016/j.actaastro.2006.04.014

Kesterson, M., Bue, G., & Trevino, L. (2006). *Wissler Simulations of a Liquid Cooled and Ventilation Garment (LCVG) for Extravehicular Activity (EVA)*. SAE Technical Paper.

Kim, Y., Lee, C., Li, P., Corner, B. D., & Paquette, S. (2002). Investigation of air gaps entrapped in protective clothing systems. *Fire and Materials*, *26*(3), 121–126. doi.org/10.1002/fam.790

Koscheyev, V. S., Coca, A., & Leon, G. R. (2007). Overview of physiological principles to support thermal balance and comfort of astronauts in open space and on planetary surfaces. *Acta Astronautica*, *60*(4–7), 479–487. doi.org/10.1016/j.actaastro.2006.09.028

Koscheyev, V. S., Coca, A., Leon, G. R., & Dancisak, M. J. (2002, December). Individual thermal profiles as a basis for comfort improvement in space and other environments. *Aviation, Space, and Environmental Medicine, 73*(12), 1195-1202. (Drewniak, Crisco, Spencier, & Fleming, 2007)

Koscheyev, V. S., Leon, G. R., & Coca, A. (2005). Finger heat flux/temperature as an indicator of thermal imbalance with application for extravehicular activity. *Acta Astronautica, 57*(9), 713–721. http://doi.org/10.1016/j.actaastro.2005.03.063

Koscheyev, V. S., Leon, G. R., & Dancisak, M. J. (2006, August 15). *Patent No. US 7,089,995 B2*.

Koscheyev, V. S., Leon, G. R., Paul, S., Tranchida, D., & Linder, I. V. (2000). Augmentation of blood circulation to the fingers by warming distant body areas. *European Journal of Applied Physiology, 82*(1-2), 103–111. doi.org/10.1007/s004210050658

Lee, Y., & Hong, K. (2013). Development of indirect method for clothing pressure measurement using three-dimensional imaging. *Textile Research Journal, 83*(15), 1594–1605. doi.org/10.1177/0040517512470193

Leon, G. R., Koscheyev, V. S., & Stone, E. A. (2008). Visual Analog Scales for Assessment of Thermal Perception in Different Environments. *Aviation, Space, and Environmental Medicine, 79*(8), 784–786. doi.org/10.3357/ASEM.2204.2008

Less EMF, Inc. (2016). *Shielding & Conductive Fabrics*. Retrieved 2016, from LessEMF.com: http://www.lessemf.com/fabric.html

Li, J., Zhang, Z., & Wang, Y. (2013). The relationship between air gap sizes and clothing heat transfer performance. *The Journal of The Textile Institute, 104*(12), 1327–1336. doi.org/10.1080/00405000.2013.802080

Lim, C. L., Byrne, C., & Lee, J. K. (2008). Human thermoregulation and measurement of body temperature in exercise and clinical settings. *Annals Academy of Medicine*

Singapore, *37*(4), 347.

Mah, T., & Song, G. (2010a). Investigation of the Contribution of Garment Design to Thermal Protection. Part 1: Characterizing Air Gaps using Three-dimensional Body Scanning for Women's Protective Clothing. *Textile Research Journal*, *80*(13), 1317–1329. doi.org/10.1177/0040517509358795

Mah, T., & Song, G. (2010b). Investigation of the Contribution of Garment Design to Thermal Protection. Part 2: Instrumented Female Mannequin Flash-fire Evaluation System. *Textile Research Journal*, *80*(14), 1473–1487. doi.org/10.1177/0040517509358796

Monchaux, N. D. (2011). *Spacesuit: Fashioning Apollo*. MIT Press.

Mundo, C. (2015, November 6). *The spacesuit of astronauts beyond technical*. Retrieved 2016, from Chismes Mundo: http://www.chismesmundo.com/el-traje-espacial-de-los-astronautas-mas-alla-de-la-tecnica/

National Aeronautics and Space Administration. (n.d.). *ILC Space Suits & Related Products*. Retrieved 2016, from NASA History Program Office: http://history.nasa.gov/alsj/ILC-SpaceSuits-RevA.pdf

National Aeronautics and Space Administration. (n.d.). *Portable Life Support System*. Retrieved 2016, from NASA: https://www.hq.nasa.gov/alsj/LM15_Portable_Life_Support_System_ppP1-5.pdf

Newman, D. J., Schmidt, P. B., & Rahn, D. B. (2000). Modeling the Extravehicular Mobility Unit (EMU) Space Suit: Physiological Implications for Extravehicular Activity (EVA). doi.org/10.4271/2000-01-2257

Nyberg, K. L., Diller, K. R., & Wissler, E. H. (2000). Model of Human/Liquid Cooling Garment Interaction for Space Suit Automatic Thermal Control. *Journal of Biomechanical Engineering*, *123*(1), 114–120. doi.org/10.1115/1.1336147

Paul, H. L., & Iovine, J. V. (1996). Extravehicular Activity (EVA) Thermal Micrometeoroid Garment (TMG) Thermal Performance Study. doi.org/10.4271/961425

Pratt, J., & West, G. (2014). *Pressure Garments: A Manual on Their Design and Fabrication*. Butterworth-Heinemann.

Psikuta, A., Frackiewicz-Kaczmarek, J., Frydrych, I. K., & Rossi, R. M. (2012). Quantitative Evaluation of air gap Thickness and Contact Area Between Body and Garment. *Textile Research Journal*, 1-9. doi.org/10.1177/0040517512436823

Meier, R. (2016). *Roger Meier's Freeware*. Retrieved 2016, from Roger Meier's Freeware: http://freeware.the-meiers.org/

Rose, N. E., Feiwell, L. A., & Cracchiolo, A. (1992). A Method for Measuring Foot Pressures Using a High Resolution, Computerized Insole Sensor: The Effect of Heel Wedges on Plantar Pressure Distribution and Center of Force. *Foot & Ankle International*, *13*(5), 263–270. doi.org/10.1177/107110079201300506

Schmidt, P. B., Newman, D. J., & Hodgson, E. (2001). Modeling Space Suit Mobility: Applications to Design and Operations. doi.org/10.4271/2001-01-2162

Seo, H., Kim, S.-J., Cordier, F., & Hong, K. (2007). Validating a Cloth Simulator for Measuring Tight-fit Clothing Pressure. In *Proceedings of the 2007 ACM Symposium on Solid and Physical Modeling* (pp. 431–437). New York, NY, USA:

ACM. doi.org/10.1145/1236246.1236308

Song, G. (2007). Clothing Air Gap Layers and Thermal Protective Performance in Single Layer Garment. *Journal of Industrial Textiles*, *36*(3), 193–205. doi.org/10.1177/1528083707069506

Strauss, S., Krog, R. L., & Feiveson, A. H. (2005). Extravehicular Mobility Unit Training and Astronaut Injuries. *Aviation, Space, and Environmental Medicine*, *76*(5), 469–474.

Tekscan. (2016). *Tekscan: Pressure Mapping, Force Measurement & Tactile Sensors*. Retrieved 2016, from Tekscan: Pressure Mapping, Force Measurement & Tactile Sensors: https://www.tekscan.com/

Wang, F., & Gao, C. (2014a). *Protective Clothing: Managing Thermal Stress*. Elsevier.

Wang, F., & Gao, C. (2014b). *Protective Clothing: Managing Thermal Stress*. Elsevier.

Wang, F., Zhu, B., Shu, L., & Tao, X. (2014). Flexible pressure sensors for smart protective clothing against impact loading. *Smart Materials and Structures*, *23*(1), 015001. doi.org/10.1088/0964-1726/23/1/015001

Watkins, S. M. (1995). *Clothing: The Portable Environment*. Iowa State University Press.

Watkins, S. M., Watkins, S., & Dunne, L. (2015). *Functional Clothing Design: From Sportswear to Spacesuits*. Bloomsbury Publishing USA.

Weber, L. (2012, July 18). *JAXA & NASA liquid cooling and ventilation garment in hot temperature desert living development opportunity*. Retrieved 2016, from Weber Luk の blog *Luk Chi Chiu Weber:

http://blog.livedoor.jp/a8712581537531/archives/5695472.html

Wong, A. S. W., Li, Y., & Zhang, X. (2004). Influence of Fabric Mechanical Property on Clothing Dynamic Pressure Distribution and Pressure Comfort on Tight-Fit Sportswear. *Sen'i Gakkaishi*, *60*(10), 293–299. doi.org/10.2115/fiber.60.293

Xu, B., Huang, Y., Yu, W., & Chen, T. (2002). *Body Scanning and Modeling for Custom Fit Garments*, 2(2), 1-11.

Xu, J., & Zhang, W. (2009). The Vacant Distance Ease Relation between Body and Garment. In *2009 Second International Conference on Information and Computing Science* (Vol. 4, pp. 38–41). doi.org/10.1109/ICIC.2009.318

Yongrong Wang, Peihua Zhang, Xunwei Feng, & Yuan Yao. (2010). New method for investigating the dynamic pressure behavior of compression garment. *International Journal of Clothing Science and Technology*, *22*(5), 374–383. doi.org/10.1108/09556221011071839

Zhang, X., Yeung, K. W., & Li, Y. (2002). Numerical Simulation of 3D Dynamic Garment Pressure. *Textile Research Journal*, *72*(3), 245–252. doi.org/10.1177/004051750207200311

Zhou, B., Cheng, J., Sundholm, M., & Lukowicz, P. (2014). From Smart Clothing to Smart Table Cloth: Design and Implementation of a Large Scale, Textile Pressure Matrix Sensor. *Architecture of Computing Systems – ARCS 2014, 8350*, 159-170.